AGU100 ADVANCING EARTH AND SPACE SCIENCE

Reviews of Geophysics

REVIEW ARTICLE
10.1029/2018RG000603

Geophysical Monitoring of Moisture-Induced Landslides: A Review

J. S. Whiteley[1,2], J. E. Chambers[1], S. Uhlemann[3], P. B. Wilkinson[1], and J. M. Kendall[2]

[1]Environmental Science Centre, British Geological Survey, Nottingham, UK, [2]School of Earth Sciences, University of Bristol, Bristol, UK, [3]Formerly British Geological Survey, now Lawrence Berkeley National Laboratory, Berkeley, California, USA

Key Points:
- Geophysical monitoring reveals high resolution spatial and temporal information from the subsurface of landslide systems
- Developments in geophysical monitoring have led to substantial increases in applications to landslides and frequencies of data acquisition
- Linking geophysical data with geotechnical measurements can monitor hydrological and geomechanical processes in time and space

Correspondence to:
J. S. Whiteley,
jim.whiteley@bristol.ac.uk

Citation:
Whiteley, J. S., Chambers, J. E., Uhlemann, S., Wilkinson, P. B., & Kendall, J. M. (2019). Geophysical monitoring of moisture-induced landslides: A review. *Reviews of Geophysics*, *57*. https://doi.org/10.1029/2018RG000603

Received 6 APR 2018
Accepted 6 NOV 2018
Accepted article online 15 NOV 2018

Abstract Geophysical monitoring of landslides can provide insights into spatial and temporal variations of subsurface properties associated with slope failure. Recent improvements in equipment, data analysis, and field operations have led to a significant increase in the use of such techniques in monitoring. Geophysical methods complement intrusive approaches, which sample only a very small proportion of the subsurface, and walk-over or remotely sensed data, which principally provide information only at the ground surface. In particular, recent studies show that advances in geophysical instrumentation, data processing, modeling, and interpretation in the context of landslide monitoring are significantly improving the characterization of hillslope hydrology and soil and rock hydrology and strength and their dynamics over time. This review appraises the state of the art of geophysical monitoring, as applied to moisture-induced landslides. Here we focus on technical and practical uses of time-lapse methods in geophysics applied to monitoring moisture-induced landslide. The case studies identified in this review show that several geophysical techniques are currently used in the monitoring of subsurface landslide processes. These geophysical contributions to monitoring and predicting the evolution of landslide processes are currently underrealized. Hence, the further integration of multiple-parametric and geotechnically coupled geophysical monitoring systems has considerable potential. The complementary nature of certain methods to map the distribution of subsurface moisture and elastic moduli will greatly increase the predictive and monitoring capacity of early warning systems in moisture-induced landslide settings.

1. Introduction

The destabilization and subsequent mass movement of soil and rock on slopes occurs across the globe, leading to loss of life and damage to property and infrastructure (Froude & Petley, 2018; Petley, 2012). Investigation of landslides can determine their key characteristics, including (but not limited to) soil and rock properties, the landslide geomorphology, types of movement, and velocity rates. Detailed knowledge of these characteristics can inform the modeling of the sensitivity of landslide masses to external triggers (Arnone et al., 2011; Jibson, 1993), which contribute to reducing risk posed by these globally occurring hazards.

The worldwide distribution of landslides is not uniform, with landslides occurring primarily where the requisite topographic, climatic, and environmental conditions are prevalent. Figure 1 shows the distribution of moisture-induced landslides (i.e., those caused by increased hydrological infiltration) recorded in the Global Landslide Catalog between 2007 and 2016 (Kirschbaum et al., 2010, 2015). An obvious pattern is the greater occurrence of landslides in areas of greater topographic variation compared to areas of relatively low relief.

High-incidence, high-fatality areas tend to be found in less developed regions (e.g., South East Asia, Central and South America) and high-incidence, low-fatality areas are generally located in more developed countries (e.g., North America, Europe). However, the Global Landslide Catalog does not capture the whole picture of landslide distribution and impact across the globe (Kirschbaum et al., 2015). In the United Kingdom, there is a well-established and maintained recording system for landslide events, operated by the British Geological Survey (Pennington et al., 2015). The United States Geological Survey has a national landslide mitigation strategy which recommends the mapping and assessment of landslide hazards (Spiker & Gori, 2003). These landslide recording programs tend to capture the occurrence of both fatal and nonfatal landslide events at many scales. However, in many other countries, particularly developing nations, such recording systems are not established, and the landslide events recorded tend to be those that have a large enough impact on life,

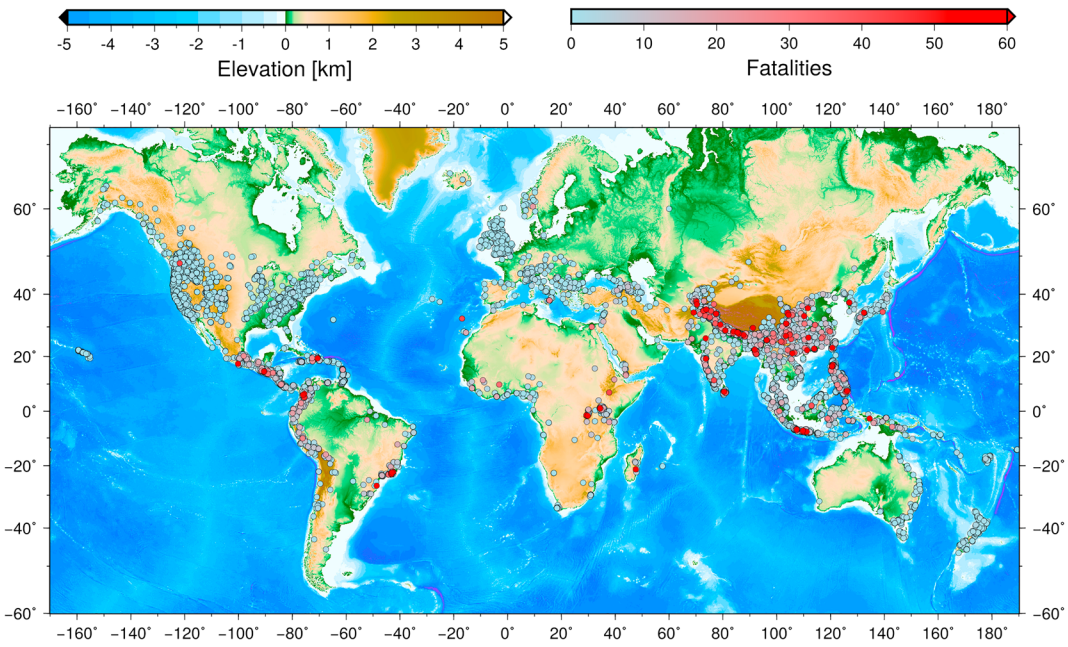

Figure 1. Global occurrences of landslides recorded in the global landslide catalog between 2007 and 2016 (Kirschbaum et al., 2010; Kirschbaum et al., 2015), including associated fatalities. Redrawn from Uhlemann (2018).

society, or the economy to be reported in the media. Although fatalities are fewer in more economically developed countries, there are still issues of completeness in reporting landslides even in Europe (Haque et al., 2016). The incidence of landslide events across the globe can therefore be taken as a lower boundary of actual landslide occurrence, and loss of life and infrastructure from landslides can be greatly underestimated in such circumstances (Petley, 2012). Landslides are often considered a secondary hazard, forming part of the problem of cascading hazards (Pescaroli & Alexander, 2015), as they are triggered by catastrophic events such as storms, floods, volcanic eruptions, and earthquakes (Gill & Malamud, 2014). This cascading effect was highlighted in Papua New Guinea in February 2018, with numerous landslides triggered by a large earthquake blocking many valleys. This valley blocking poses a continuing flood risk as water builds up behind these unstable structures with increased seasonal rainfall.

The term "moisture-induced landslides" (MIL) is used in this review to refer to landslides triggered by increased water infiltration. Elevations in subsurface moisture content can be caused by extended periods of increased infiltration, or by increased volumes of water. Most infiltration in landslide settings comes from increased precipitation or snowmelt, and due to the complex role of evapotranspiration, the amount of rainfall or snowmelt that reaches the subsurface can vary throughout the climatic cycle. The amount of moisture that does reach the subsurface is known as "effective infiltration." Therefore, the term MIL recognizes the multiple sources of moisture that affect landslides, the importance of the concept of effective infiltration, and its subsequent effect on the instability of materials in response to moisture infiltration.

The advances in hardware and software for geophysical monitoring reflect those made in remote sensor technology, mainly in the ability to deploy increasingly low-cost and low-power sensors to capture information from the subsurface with a minimal delay in data acquisition and transmission (Ramesh, 2014). The main benefit arising from these developments has been the increase in monitoring durations achieved by the installation of permanent sensors (Ramesh & Rangan, 2014). However, geophysical monitoring approaches have the added benefit of providing increasingly high-resolution spatial information.

This review appraises the state of the art of the application of geophysical methods to monitoring moisture-induced landslides. Geophysical monitoring provides information on fundamental subsurface slope process, and is relevant to those studying landslides and their behavior. However, this information can also be vital to those looking to mitigate landslide hazards, and in particular, can provide information on precursory failure conditions in unstable slopes. Therefore, the content of this review is also of interest to early warning systems (EWS) operators looking to incorporate spatial and temporal subsurface data into their monitoring systems.

In this review, "geophysical methods" specifically refer to surface deployed techniques to investigate features in the shallow subsurface. The term "monitoring" is used to indicate a time-lapse approach to investigate changes between two or more geophysical data sets acquired at the same location at different times. Recent literature shows two main methods being employed for the monitoring of landslides, geoelectrical and seismic. The relevance of geophysical monitoring to landslides is addressed by first identifying landslide characteristics and the application of geophysical methods. A review of case studies of geophysical monitoring of landslides is then undertaken in light of the methods currently in use. Finally, recommendations for the use of geophysical methods in the monitoring of landslides will be revisited in the context of slope-scale EWS.

2. Landslide Settings and Processes: Definitions

The most longstanding and recognized classification of landslides is that of Cruden and Varnes (1996). This classification system has been updated in recent years to reflect modern standards of material properties (Hungr et al., 2014). Other well-established and regularly used systems exist for other specific landslide types (e.g., Fell, 1994; Leroueil et al., 1996; Skempton & Hutchinson, 1969). The updated Cruden and Varnes (1996) system by Hungr et al. (2014) comprehensively outlines the types of movement, the geological materials, and velocities of material movement that describe the majority of landslide occurrences across the globe.

For this review, it is useful to distinguish between the spatial definition of a landslide setting, and the temporal description of the evolving processes of movement:

1. The "landslide setting" is the spatial definition of a geographical area that may be prone to, or have experienced, the downslope mass movement of geological material (e.g., Jongmans et al., 2009). Characteristics of the landslide setting would include the geological materials (rock, boulders, debris, sand, clay, silt, mud, peat, ice) as well as the geomorphology of the unstable slope (Guzzetti et al., 1999; Hungr et al., 2014).
2. "Landslide processes" indicate the onset and subsequent processes of movement of unstable geological material in time (e.g., Hutchinson & Bhandari, 1971). These include the changes in the subsurface conditions of landslides preceding observable failure, such as elevations in pore water pressure that may induce future movement in landslides. These processes may be difficult to measure, and often can only be inferred by observing changes in a property (e.g., ground moisture) over time. Factors relating to landslide processes would include the types of movement (flows, topples, slides, spreads, and deformations), velocities of movement ($<$16 mm/year to $>$5 m/s; Hungr et al., 2014), and the hydrogeological and geomechanical processes acting upon the landslide materials.

Identification of the affected area is typically undertaken by walk-over surveys, studying of aerial photographs, or via other remote sensing methods such as satellite imagery (Carrara et al., 1992, 2003; Guzzetti et al., 2012). Landslide investigations using geotechnical means typically involve identification of the three-dimensional subsurface structure of the landslide, the definition of the hydrogeological regime, and the detection of movement in the landslide mass (Mccann & Forster, 1990). This has traditionally been undertaken with intrusive investigation methods, such as the use of trial pits and boreholes to recover samples and identify changes in materials and their properties within the body of a landslide (Angeli et al., 2000; Uhlemann, Smith, et al., 2016). These approaches allow for a great amount of detailed information to be gathered at discrete locations. However, due to the heterogeneous subsurface conditions of landslide settings and the dynamic response of landslide processes to external influences, they are not always adequate in providing a wider view of the landslide system, both spatially and temporally.

3. Landslide Geophysics: An Overview

Investigations of subsurface landslide features are necessary to provide the input for forward modeling and subsequent predictions of potential failure events, for example, estimating the runout length, the mobilized volume, or the velocity of a potential failure event (Malet et al., 2005; Rosso et al., 2006). In general, geophysical techniques identify spatial variations of a physical parameter of the subsurface, from which inferences on a range of processes and properties can be made (Everett, 2013; Kearey et al., 2001; Parsekian et al., 2015). When applied to landslide investigation, geophysical techniques are able to target characteristics and features of landslide settings that are manifested by physical property contrasts in the subsurface (Mccann & Forster, 1990), including the following:

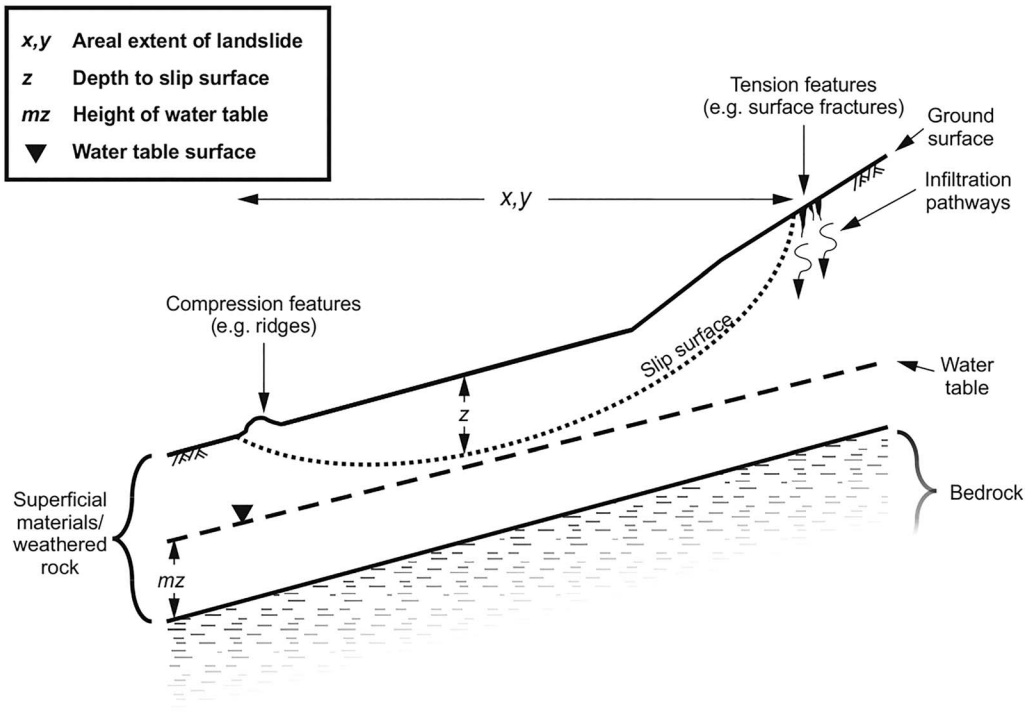

Figure 2. Schematic of a landslide system, showing the major landslide setting features that can be investigated and assessed using geophysical methods.

1. The physical extent of the landslide, comprising critical features such as the subterranean slip surface and water table
2. Variations in lithological and soil units
3. Variations in distribution and movement of moisture throughout the landslide body
4. Variations in the geomechanical strength of the landslide body

3.1. The Landslide Setting and Geophysical Investigation

The features of a typical landslide system that can be identified and assessed using geophysical methods are shown in Figure 2. These features are typified by the existence of a physical discontinuity (e.g., slip surface, lithological contact) or a contrast in material properties (e.g., degree of saturation, clay content) being present in the subsurface. Table 1 summarizes the main landslide features identified in Figure 2, and lists the targeted discontinuity or property contrast, and the applicable geophysical techniques for identifying these features.

3.2. Landslide Processes, Soil Mechanics, and Geophysical Investigation

The major parameters influencing slope stability are summarized in Figure 3. This summarizes the classical understanding of slope failure through the principles of soil mechanics (Terzaghi, 1943; Terzaghi et al., 1996), indicating the key geotechnical parameters acting upon unstable slopes. The figure is a simplified model of a slope, making many assumptions, such as the length of the slope, but indicates the main property to consider when estimating slope stability. The Mohr-Coulomb failure criterion (Terzaghi, 1943) determines the shear strength (τ_f) of the material at a given point at the slip surface interface, and is given by

$$\tau_f = c + (\sigma - u)\tan\phi'_{cv}, \tag{1}$$

where c is the cohesion, σ is the total normal stress, u is the pore water pressure, and ϕ'_{cv} is the angle of shear resistance at a critical state.

The total normal stress (σ) is given by

Table 1
Summary of the Landslide Features Able to be Identified, Assessed, and Investigated Using Geophysical Methods

Feature of the Landslide Setting	Discontinuity or Property Contrast	Applicable Geophysical Methods	Example
Landslide extents (x, y, z)	Slip surface (subsurface and surficial extent) caused by or indicated by changes in density, water content, etc., of material	Electrical resistivity, seismic reflection, seismic refraction, surface wave methods, ground-penetrating radar	Chambers et al. (2011)
Subsurface material type and structure	Material density	Microgravity	Sastry and Mondal (2013)
	Relative degree of saturation	Electrical resistivity, electromagnetics	Springman et al. (2013)
	Relative clay content	Electrical resistivity, electromagnetics	Göktürkler et al. (2008)
	Material velocity (as a function of density)	Seismic reflection, seismic refraction, surface wave methods	Renalier, Jongmans, et al. (2010)
Water table	Height of water table	Electrical resistivity, electromagnetics, seismic refraction	Le Roux et al. (2011)
	Relative flow direction	Self-potential	Perrone et al. (2004)
Tension features (e.g., surface fractures)	Saturation contrasts (e.g., preferential infiltration pathways)	Electrical resistivity, electromagnetics, ground-penetrating radar, self-potential	Bièvre et al. (2012)
Compression features (e.g., ridges)	Variations in material composition	Electrical resistivity, electromagnetics, ground-penetrating radar	Schrott and Sass (2008)

$$\sigma = \{m\gamma + m\gamma_{sat}\}z\cos^2\beta, \tag{2}$$

where m is the height, γ is the unit weight of material, γ_{sat} is the saturated unit weight of material, z is the depth to slip surface, and β is the slope angle. Shear stress (τ) is given by

$$\tau = \{m\gamma + m\gamma_{sat}\}z\sin\beta\cos\beta. \tag{3}$$

The pore water pressure (u) at the slip surface is calculated by

$$u = mz\gamma_w\cos^2\beta. \tag{4}$$

In order for slope failure to occur, the restraining forces, in this case shear strength (τ_f), must be overcome by disturbing forces, or shear stress (τ). This can be expressed in terms of a factor of safety (*FoS*), given by

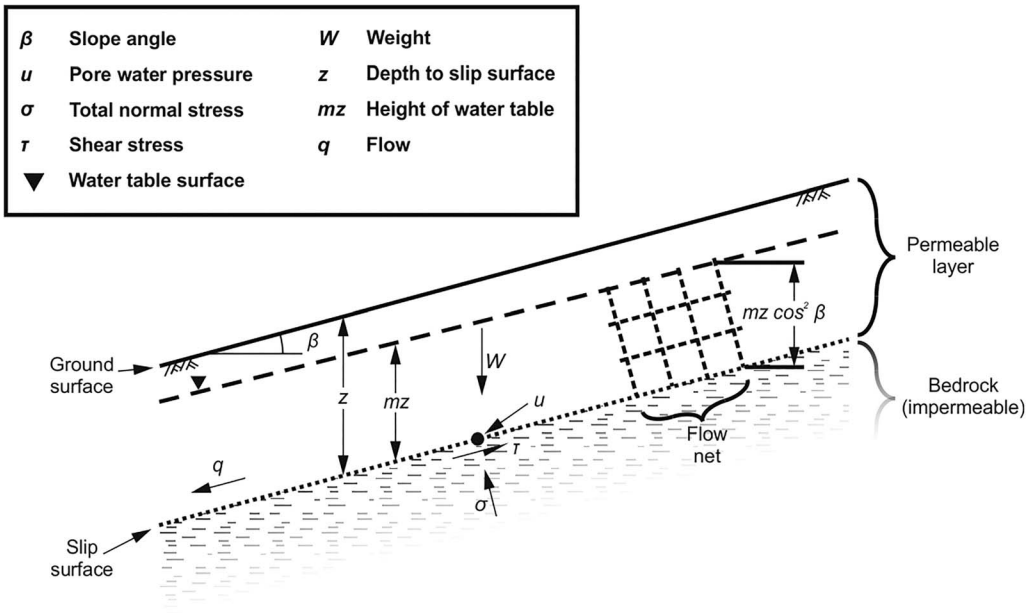

Figure 3. Schematic of an infinite slope model showing the main landslide processes showing the main components of a classical soil mechanics approach to slope failure (Terzaghi, 1943), redrawn from Craig (2004).

Table 2
Parameters of Landslide Processes That Can Be Investigated Using Geophysical Methods

Slope Stability Property	Investigable Feature	Applicable Geophysical Methods	Example
Normal stress (σ) $\boldsymbol{\sigma = \{m\gamma + m\gamma_{sat}\}z\cos^2\beta}$	Depth to slip surface (z)	Electrical resistivity, seismic reflection, seismic refraction, surface wave methods, ground-penetrating radar	Renalier, Jongmans, et al. (2010)
	Relative proportions of dry (or partially saturated) material ($(1-m)\gamma$) Relative proportions of saturated material ($m\gamma_{sat}$)	Electrical resistivity, seismic reflection, seismic refraction, ground-penetrating radar	Grandjean et al. (2010)
Pore water pressure (u) $\boldsymbol{u = mz\gamma_w\cos^2\beta}$	Height of water table (mz)	Electrical resistivity, seismic reflection, seismic refraction, ground-penetrating radar	Sastry and Mondal (2013) and Grelle and Guadagno (2009)
Cohesion (c)	Presence of clay in subsurface material	Electrical resistivity, ground-penetrating radar	Göktürkler et al. (2008)
Shear strength (τ_f) $\boldsymbol{\tau_f = c + (\sigma - u)\tan\phi'_{cv}}$	Estimates of angle of shear resistance at critical state (φ'_{cv}) can be made using back analysis from estimating σ and u	Seismic refraction, surface wave methods	Al-Saigh and Al-Dabbagh (2010)

$$FoS = \frac{\tau_f}{\tau}. \tag{5}$$

When $FoS < 1$ slope failure will occur, with $FoS > 1$ indicating stable slope conditions. $FoS < 1$ can be reached by increasing τ, for example, by greater loading on the slope, or by reduction in τ_f, for example, by increasing u (equation (1)). Not highlighted in these equations is the critical role that negative pore water pressures, or soil suction (or matric suction) can play in the stabilization of landslide bodies (Toll et al., 2011). Materials with larger void spaces, such as sands and gravels, will have smaller capillary zones (the area of saturation above the water table caused by soil suction) than cohesive materials with smaller void spaces such as clays and silts (Craig, 2004). In some slopes, soil suctions may be the main restraining force preventing failure (Hen-Jones et al., 2017). In these settings, understanding of subsurface moisture dynamics relating to increased infiltration is critical for predicting future slope failures.

In a geophysical survey, the result may determine the presence or extents of a landslide property (e.g., the water table). This time-static geophysical data set gives information on the state of one (or more) property in the system at that particular time, but not how that property will change in response to some external influence (e.g., precipitation). With the addition of a second geophysical data set at some point in the future, it may be possible to determine a change in that property (e.g., increase in water table height). The implicit assumption is that in order for a property change to have occurred, a process must have taken place in the time between the two surveys (e.g., infiltration). By looking at the differences between the data at each end of the time period, reasonable inferences can be made about the process that must have occurred to give rise to a change in the system.

Therefore, geophysical methods used in isolation are not able to definitively quantify the contributions that changes in these properties make to the overall stability of a slope, but the incorporation of environmental data (e.g., rainfall data) and the use of geotechnically coupled surveys can provide empirical relationships that allow for such contributions to be assessed. Table 2 shows the parameters of landslide processes to which various geophysical methods are sensitive.

The figures presented in this section are simplified versions of landslide systems, meant to illustrate the features on landslide settings and processes that can be investigated in some way using geophysical methods. Field conditions are likely to present more heterogeneous conditions than those represented here. However, the identification of such heterogeneous conditions is itself an advantage of using geophysical methods to investigate landslide, with the spatial coverage of geophysical methods being one of the main benefits of the techniques (Everett, 2013; Kearey et al., 2001).

3.3. Applications of Geophysical Methods to Landslide Investigation

For a geophysical methodology to be effective as a monitoring tool, several criteria must be fulfilled:

1. The subsurface property or process (e.g., moisture content) being measured or monitored must be detectable by the chosen method.
2. The acquisition rate of data must be sufficiently high (with respect to changes in the monitored process) so as to be able to collect data sets which sample physical property changes at an appropriate rate.
3. The measuring equipment must be able to be relocated accurately for series of discrete fieldwork campaigns, or the position of geophysical sensors must be accurately located if a semipermanent installation is established.
4. The data must ideally be able to be empirically linked to subsurface conditions so as to confidently reflect the changes that occur in the physical properties of the subsurface over time.

In recent years, the application of geophysical methods to the characterization of landslide settings has become increasingly common. Hack (2000) outlined the physics underpinning geophysical surveys for slope stability analyses, and Jongmans and Garambois (2007) provided a review of published landslide investigations using geophysical methods since the mid-1990s.

Both of these reviews highlight three important developments in landslide geophysics: the integration of multiple methods, the acquisition of multidimension data (including time-lapse approaches), and the quantification of geophysical results with geotechnical data. The integration of multiple geophysical methods for landslide investigations has become more common in recent years, allowing for better evaluation of internal structure to be made by overcoming the limitations of single-technique approaches (Schrott & Sass, 2008). However, multiple-method approaches to landslide monitoring using geophysical methods are still relatively scarce (Jongmans & Garambois, 2007).

The spatial dimensions across which geophysical data can be acquired have increased over time. One-dimensional (1-D) "sounding" type data provides information on the subsurface beneath a single location on the ground surface. These vertical profiles of information can be interpolated to form pseudo-two-dimensional and pseudo-three-dimensional data sets of subsurface properties.

True two-dimensional (2-D) survey techniques allow data to be collected spatially across the ground surface (also referred to as "geophysical mapping"), or as a subsurface profile or cross section. The latter of these techniques can be interpolated to produce pseudo-three-dimensional volumes of data. True three-dimensional (3-D) surveys involve the simultaneous acquisition of volumes of data. All of these dimensions of data acquisition produce a static map of the distribution of physical properties within a landslide body, and prove invaluable for the characterization of landslide settings. However, in order to work toward the prediction of landslide failure, an investigation method that takes into account the temporal variation within the landslide system should be used.

Geophysical techniques that include the addition of a time series to the acquired data are sometimes referred to as "time-lapse" or "4-D" data sets. As 4-D specifically refers to a 3-D data set with multiple time steps, the term time lapse will be used in this review to refer to data sets of any dimension (1-D, 2-D, and 3-D) which include multiple time steps. Time-lapse geophysical monitoring of landslides is an area that has grown rapidly in the last decade or so (Jongmans & Garambois, 2007).

In order for the application of geophysical techniques to the monitoring of MIL over time to be successful, the frequency of data set acquisition must be proportional to the time scale over which changes occur in the subsurface properties of the landslide. Geophysical monitoring therefore lends itself to the monitoring of slowly deforming slopes. These slopes are typically composed of highly weathered rocks or soils and other superficial materials (such as tills, alluvium, and other recently reworked materials). Failure in these landslide environments can be both "brittle" (i.e., failure occurs along discreet shear surfaces) or "ductile" (i.e., the deformation processes are slow, such as slope creep). Landslides triggered by increased infiltration of water are of particular interest to geophysicists, as the formation and progression of precursory failure conditions can be detected using geophysical data, processing, and interpretation (Baroň & Supper, 2013). For this reason, fast-failing and fast-moving landslides that do not typically exhibit gradual changes in subsurface properties prior to failure have been excluded from this review. These landslide types are typically fast-failing rockfalls and rock topples, fast-moving debris flows, and fast-failing and fast-moving rock avalanches (Hungr et al., 2014). In some instances, these types of failure may also be present in a MIL setting (e.g., Helmstetter & Garambois, 2010; Lacroix & Helmstetter, 2011) It is important to note, however, that geophysical monitoring systems do exist for these types of failure (Fiorucci et al., 2016; Lotti et al., 2015;

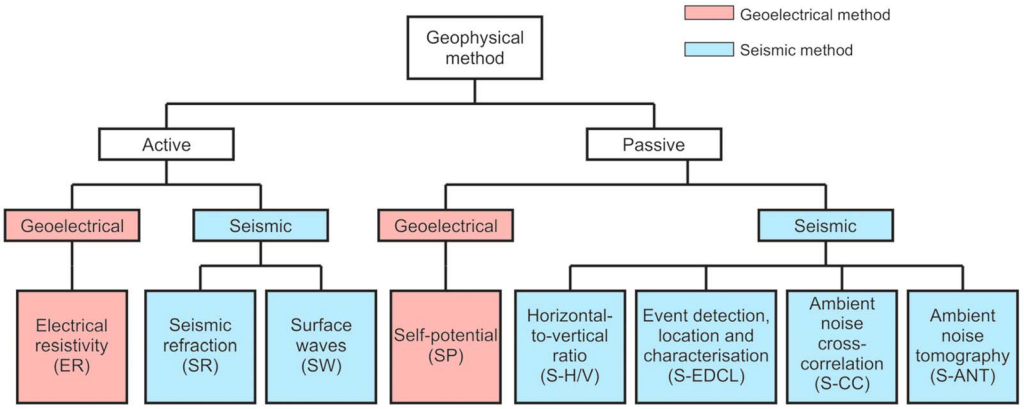

Figure 4. The geophysical methods identified in the 31 case studies, shown by mode of acquisition and method. The acronyms for each method are shown in the lower boxes.

Partsinevelos et al., 2016) and that many of the geophysical methods described here are similar in their application to these failure types. The case studies presented in this review therefore have a focus on the monitoring of landslides in settings comprising of soft-rock and superficial materials.

MIL are typically shallow, translational, and/or rotational style landslides, with failure frequently occurring in soils and weathered bedrock layers. An exception to this is deep-seated gravitational slope deformation-type failures, which are characterized by very slow deformations of very large rock masses (Jomard et al., 2010; Lebourg et al., 2005). These have been included in this review as the progression of failure is slow enough to be robustly monitored using geophysical approaches, and periods of increased movement are linked to increases in precipitation (Helmstetter & Garambois, 2010; Lacroix & Helmstetter, 2011; Palis, Lebourg, Vidal, et al., 2017). The study of landslides and their evolving processes is a highly interdisciplinary area of research. As such, the application of monitoring MIL has important implications for geologists, geomorphologists, geotechnical engineers, and infrastructure stakeholders, especially as the impact of climate change is having a dramatic effect on the incidence of slope failures due to changing weather patterns (Gariano & Guzzetti, 2016).

4. Geophysical Monitoring of Landslides: Methods and Case Studies

A list of publications in scientific journals and books since 2006 that utilize geophysical monitoring applied to landslides is shown in Appendix A. In total, 38 journal articles or book chapters are identified as using or describing geophysical monitoring approaches in landslide systems. Of these 38 publications, two are project updates that do not contain data, and 36 describe specific case studies. Some of the individual monitoring campaigns are described in more than one publication, and where possible this is indicated, leaving a total of 34 publications. Within these 34 publications, 54 monitoring campaigns at 27 separate landslides are identified from nine countries.

The geophysical monitoring methods identified and their corresponding abbreviations for this paper are shown in Figure 4. Further descriptions of these methods are found in the relevant sections detailing the case studies. Two broad types of geophysical methods are identified from this list: geoelectrical and seismic methods. In addition, two modes of acquisition are identified in both types: "active" modes, in which the recorded geophysical signal is artificially generated, and "passive" modes, in which the signal recorded is generated naturally.

In geoelectrical methods one active type, electrical resistivity (ER), and one passive type, self-potential (SP) monitoring, are identified. Typically, 2-D electrical resistivity (ER) profiles are acquired as part of the study, with similar instrumentation, acquisition parameters, processing routines, and inversion methods applied across the case studies. Some examples where geoelectrical data sets are manipulated in bespoke ways do exist, for example, the use of apparent resistivity (Palis, Lebourg, Tric, et al., 2017), transfer resistance data (Merritt et al., 2018), and 3-D ER arrays (Uhlemann et al., 2017). The use of SP methods is also noted, although in a much reduced capacity to ER (Colangelo et al., 2006). In total, 20 time-lapse ER monitoring surveys are

identified in the literature: Bièvre et al. (2012), Crawford and Bryson (2018), Friedel et al. (2006), Gance et al. (2016), Grandjean et al. (2009), Jomard et al. (2007), Lebourg et al. (2010), Lehmann et al. (2013), Lucas et al. (2017), Luongo et al. (2012), Merritt et al. (2018), Palis, Lebourg, Vidal, et al. (2017), Palis, Lebourg, Tric, et al. (2017), Supper et al. (2014), Travelletti et al. (2012), Uhlemann et al. (2017), and Xu et al. (2016). One time-lapse SP monitoring survey is identified, by Colangelo et al. (2006).

In seismic methods, the active types of surveying include seismic refraction (SR) and analysis of surface waves (SW) and the passive types include seismic event detection, characterization, and location (S-EDCL); seismic cross correlation (S-CC); seismic horizontal-to-vertical ratio (S-H/V); and seismic ambient noise tomography (S-ANT). One study by Grandjean et al. (2009) used SR monitoring, and a study by Bièvre et al. (2012) utilized SW monitoring methods. In total, 31 case studies are identified as using passive seismic methods: Amitrano et al. (2007), Brückl and Mertl (2006), Brückl et al. (2013), Gomberg et al. (2011), Harba and Pilecki (2017), Imposa et al. (2017), Mainsant et al. (2012), Palis, Lebourg, Vidal, et al. (2017), Provost et al. (2017), Renalier, Jongmans, et al. (2010), Tonnellier et al. (2013), Walter and Joswig (2008), Walter et al. (2009), Walter et al. (2011), Walter et al. (2012), and Walter et al. (2013).

Some geophysical methods are absent from the literature surrounding landslide monitoring; for example, no studies in which ground penetrating radar has been used as a long-term monitoring tool are identified, although it has been used to provide detailed qualitative characterization of landslide settings (Hruska & Hubatka, 2000).

Before presenting the details of individual methods and case studies, it is helpful to consider the different conditions under which the geophysical monitoring campaigns listed in Appendix A were acquired. The most important aspects of these conditions to consider are the duration of monitoring, the modes of acquisition, and the frequency at which data were acquired during the campaign.

4.1. Duration of Geophysical Monitoring Data Acquisition

The durations of geophysical monitoring were able to be divided in to four approaches:

1. *Controlled tests*: Typically artificial infiltration-type experiments in which an unstable slope was exposed to an increase in saturation by introducing simulated rainfall over a set period of time and subsurface conditions monitored throughout. Although the field instrumentation remained static between acquisitions, the field setups were not typically designed for long-term monitoring, and were assumed to have been accompanied by field crew for the duration of the experiment. The shortest and longest controlled experiments were both described by Lehmann et al. (2013), at 15 hr in one test and three days in another. All controlled experiment case studies showed a high-frequency of data set acquisitions, typically every few hours. Six controlled tests were described in five publications: Grandjean et al. (2009), Jomard et al. (2007), Lehmann et al. (2013), Travelletti et al. (2012), and Colangelo et al. (2006).
2. *Transient measurements*: Typically involved the deployment of instruments for the duration of a single data set acquisition, after which the instrumentation was removed from the field before being deployed again in the same location after a period of time. Monitoring periods varied greatly, with the shortest recorded as 62 days (Lucas et al., 2017) and the longest as 1589 days (Imposa et al., 2017). In both of these studies, six data sets were acquired over the monitoring period, highlighting the variability in acquisition frequency that can accompany a transient measurement approach.
3. *Short-term installations*: Utilize equipment installed and left in the field, but for shorter periods than semipermanent installations. Consequentially, the length of these monitoring campaigns fall between controlled tests and semipermanent installations. Unlike controlled tests, environmental conditions are not artificially altered (e.g., by artificial rainfall), and instead, natural variations in environment and subsurface response are monitored. However, equipment tends to be deployed for periods of less than 100 days, and so surveys cannot typically monitor seasonal- or annual-scale variation subsurface conditions, although the monitoring period may coincide with periods of increased rainfall. Often, the full cycle of a monitoring campaign may involve several short-term installations at the same landslide (e.g., Brückl & Mertl, 2006), although in some studies, the exact position can vary between these repeated surveys (e.g., Walter et al., 2011). The shortest period of monitoring using short-term installations was for one day, although this day comprised one survey of a sequence described by Brückl and Mertl (2006). The longest period of monitoring achieved with a short-term installation was by Lebourg et al. (2010) at 90 days.

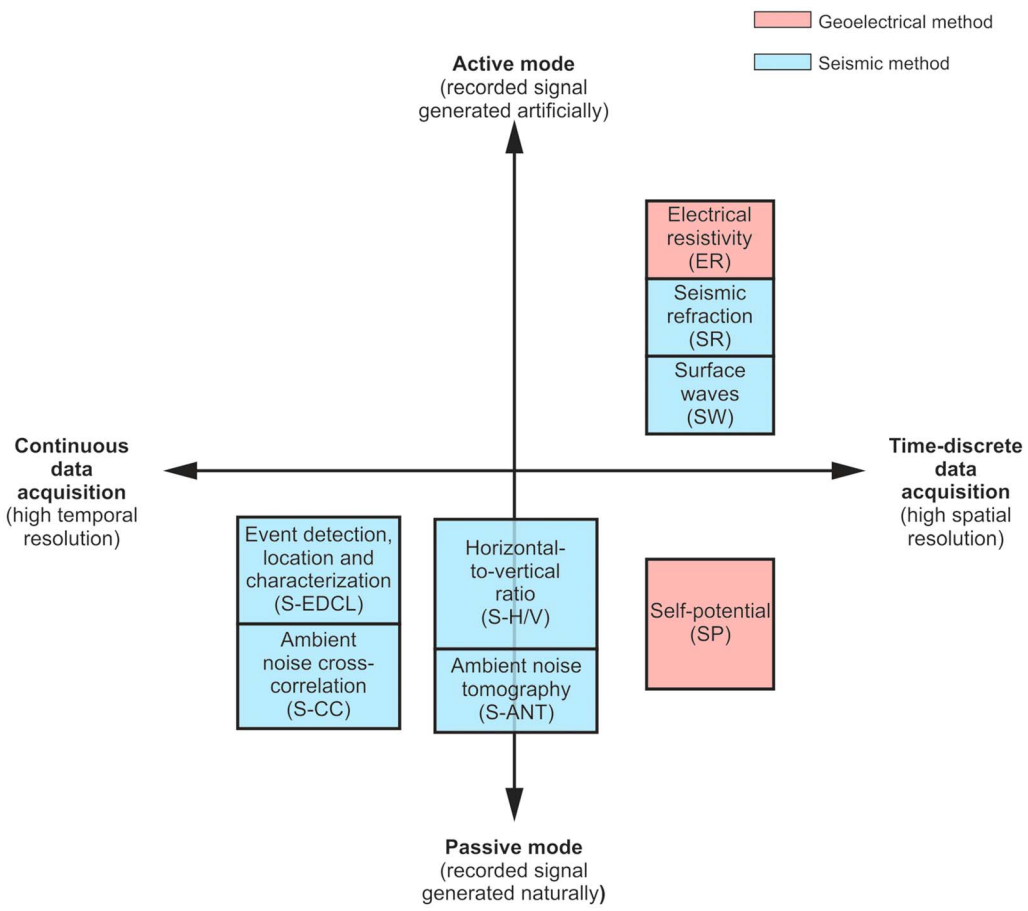

Figure 5. Relationship between the geophysical methods outlined in Appendix A in terms of their acquisition mode (active or passive) and temporal resolution (continual or time-discreet) demonstrating the trade-offs which must be considered when choosing a method for monitoring of MIL.

4. *Semipermanent installations*: Installations are left in the field to acquire data according to a predetermined (or sometimes remotely programmable) schedule. Unlike transient measurements, the time period between acquisitions was often regular. Semipermanent installations allow for a high-frequency data acquisition (typically one or more data sets acquired per day) over long monitoring periods (typically months to years). The shortest monitoring period studied with a semipermanent installation was 146 days in a study by Luongo et al. (2012). Most studies operating at annual-scale time periods, and often at an acquisition rate of more than one data set per day. In Supper et al. (2014), two examples are given, where data sets were recorded every 4 hr for 239 and 275 days at two separate sites. These monitoring systems also tend to include the ability for data to be retrieved remotely from the equipment, often by utilizing telemetry and storage of data on a remote server.

4.2. Acquisition Mode of Geophysical Monitoring Data

Figure 5 shows the relationship between different geophysical methods, and how they are suited to different types of geophysical monitoring. Geophysical methods acquiring active mode data lend themselves to acquiring higher-resolution spatial data due to the tendency toward acquiring time-discreet data sets. Geophysical methods acquiring passive mode data tend to higher-resolution temporal data, as they acquire temporally continuous data sets. Some geophysical methods, however, are able to produce high-resolution spatial data from passive acquisition modes.

4.3. Geophysical Data Acquisition Frequency

Figure 6 shows a chart plotting the duration of each monitoring campaign against the number of data sets acquired in each monitoring campaign. There is some difficulty equating the number of data sets acquired

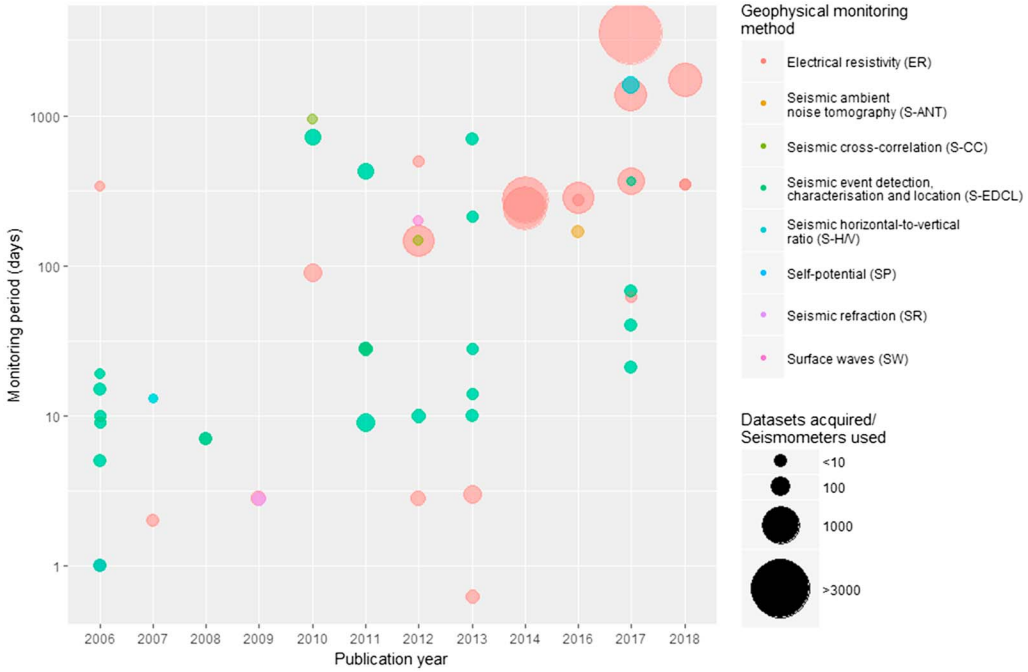

Figure 6. Plot showing the year of publication for case studies against the number of days in the monitoring period for each case study. The relative area of each data point is proportional to the number of data sets acquired. Data collected from seismic monitoring networks are considered to have collected one data set per sensor for the entire monitoring period.

in a monitoring period between different types of geophysical methods. The ER, SP, SR, SW, S-ANT, and some S-H/V methods acquire time-discreet sets of data. This is because the entirety of a data set is made up of a multitude of unique data points, the position and number of which determine the spatial resolution of the survey method. These methods therefore tend to have high spatial resolution and coverage (see Figure 5). It is the number of electrodes (in ER and SP surveys), geophones (in SR and SW surveys), or seismic sensors (in S-ANT and S-H/V surveys) that define the spatial resolution and coverage; the more measuring points to the system, the higher the resolution and/or the larger the spatial coverage of the monitoring system. However, the temporal resolution is limited to the amount of time it takes to acquire the full complement of unique readings in a whole data set. In ER systems, for example, it can take several hours for a full data set to be acquired.

In contrast, S-EDCL, S-CC, and some S-H/V methods acquire data from continually recording seismometers. In these cases, data are acquired for the entirety of the monitoring period, with the exception of any periods of maintenance or failure. These methods therefore have high temporal resolution (see Figure 5); however, similarly to discreet data set acquisition systems, the spatial resolution is still dependent on the number of measuring components. For some applications (e.g., S-CC and S-H/V), data are divided into daily records, but in some methods (e.g., S-EDCL), only the time of the event recorded is required. The number of data sets acquired in a monitoring period by seismometers is therefore technically one data set per field campaign, although this can be completely arbitrary in some processing methods. In some approaches, such as in S-ANT, the distinction between continuously acquired and time-discreet data is blurred further, as the data processing typically deals with discrete time steps extracted from the continuous data set.

Therefore, in Figure 6, for time-discreet data set acquisition systems (ER, SP, SR, SW, S-ANT, and some S-H/V methods), the number of data sets acquired across the entire monitoring period are plotted. For monitoring campaigns that utilize continually recording seismometers (S-EDCL, S-CC, and some S-H/V methods), the number of seismometers, rather than the number of data sets acquired, has been plotted. For seismometer entries, this therefore gives an indication of the spatial resolution of the survey, rather than the temporal resolution, which can be assumed to be total for the monitoring period.

With regards to the spatial resolution and coverage of surveys, an ER system for example, may have a single unit (with a single data logger, single power source, single telemetric communication system) controlling an entire electrode array consisting of several tens of electrodes, across a profile of hundreds of meters. Conversely, a single seismometer, or localized array of seismometers, is typically operated by a single logger with a single power source and the coverage of data acquisition is dependent on the events detected at that location. To expand the spatial resolution, a second seismometer with a separate logger and power source must be added. In contrast, expanding the spatial coverage of an ER monitoring system may be as simple as adding extra electrodes in to the system.

Figure 6 illustrates several interesting developments in the field of geophysical monitoring of MIL in the last decade or so. First, the number of published studies is increasing in time, suggesting increases in the application of geophysics to landslide monitoring, or in some cases, the recent maturation of long-term studies. Second, there is a notable increase in ER case studies from 2012, and a sharp increase in both the monitoring period lengths and amount of data collected by these studies. This suggests greater developments in the field of monitoring landslides using ER methods, compared to seismic methods which show much more restrained increases. This trend is curious, as passive seismic instrumentation has been at a far more advanced state of development for long-term monitoring for much longer than ER methods.

4.4. Geoelectrical Monitoring Case Studies

Moisture dynamics can vary greatly over time, although lithological composition tends to remain relatively constant, particularly in a prefailure condition. Geoelectrical monitoring can therefore be used for the determination of moisture dynamics and hydrogeological processes within MIL bodies over time.

4.4.1. Active Geoelectrical Methods

4.4.1.1. ER

Electrical resistivity (ER) is a common technique routinely applied to the investigation of landslides (Jongmans & Garambois, 2007). The method can be applied in 1-D, 2-D, and 3-D investigations (Loke et al., 2013), although 2-D and 3-D investigations of landslides are more common in recent times. ER is measured by injecting a DC current into the ground between two electrodes, and measuring the potential difference between a separate pair of electrodes (Kearey et al., 2001). By deploying linear arrays of electrodes, measurements can be made using different combinations of electrodes in order to build a 2-D image of the subsurface resistivity. Similarly, 3-D data sets can be acquired using multiple parallel (and orthogonal) profiles or grids of electrodes.

In a typical 2-D linear array, the number of unique measurements made is proportional to the number of electrodes deployed at the ground surface. The position of a single resistivity measurement is a function of the distance between the electrodes used, and their position on the ground surface. In most near-surface geophysical applications, the raw data recorded by ER meters ("apparent resistivity") is processed using a tomographic inversion. The process of tomographic inversion produces a ground model based on the data recorded and a set of assumptions made from physical laws (e.g., current flow through subsurface equipotential surfaces) and Earth observations (e.g., subsurface models obeying geological principles). Crucially, the process provides information between the measurement points of an array based on the surrounding data. Inversions can be done in 2-D and 3-D, and with the addition of time-lapse sequences in which the time series between data set acquisitions is treated as a variable in the inversion process. However, a common approach is to undertake separate inversions of data at individual time step, and create difference models (e.g., percentage changes or difference ratios) between the results. This approach, while less computationally expensive, can omit or exaggerate important features that may be highlighted by a true time-lapse inversion.

The result of any inversion is typically an image showing the distribution of resistivity in the subsurface. The full process from acquisition to inversion is often referred to interchangeably as electrical resistivity tomography or electrical resistivity imaging. Tomographic inversion can be computationally expensive, and for this reason, ER data are occasionally not inverted to produce images of the subsurface. Alternative uses of ER data include assessing the raw measurements, or apparent resistivity, visually and statistically to detect changes in the subsurface over time. Another use of noninverted data is to look at transfer resistances between electrodes in an array. These measurements do not divulge information on spatial variations in the resistivity data, but are still sensitive to changes in moisture content over time. The advantage of these approaches is the rapidity of assessments that can be made with minimal manual interpretation and computing resources.

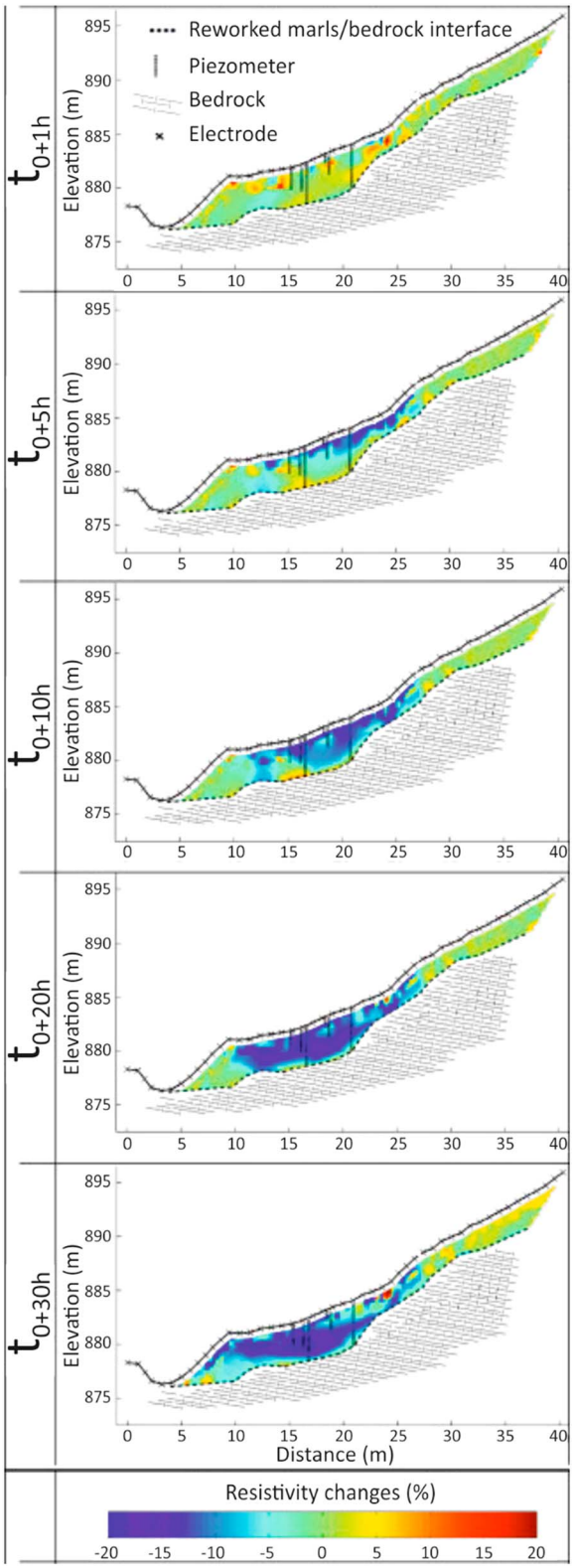

Figure 7. The results of a controlled test time-lapse ER survey by Travelletti et al. (2012) under artificial rainfall conditions (see text). The inverted ER images showing a decrease in resistivity in response to the increased saturation of the subsurface. Modified from Travelletti et al. (2012). Copyright © 2011 by John Wiley & Sons, Inc. Reprinted by permission of John Wiley & Sons, Inc.

In the case study publications identified in Appendix A, 17 of the surveys used time-lapse ER methods; five were under controlled test conditions, four utilized transient measurements, and eight described semipermanent installations of electrode arrays. In most of the studies, the stated aim of the time-lapse ER surveys was to identify properties pertaining to water movement or distribution within the landslide setting. These studies were all undertaken in 2-D, with the exception of one time-lapse ER survey that was undertaken in 3-D (Uhlemann et al., 2017).

In one controlled test case study by Travelletti et al. (2012), simulated rainfall was applied to a 100-m^2 area of the accumulation zone in the Laval landslide, South French Alps. A 47-m-long profile comprising 48 electrodes spaced 1 m apart collected electrical resistivity data over a 67-hr period of artificial rainfall of 11 mm/hr. The experiment started under unsaturated conditions (at approximately 27% saturation) and aimed to determine the time at which steady state flow was reached in the landslide body. By comparison with piezometer data, this was determined to have occurred 21 hr after the onset of artificial rainfall. The results of the time-lapse ER survey are shown in Figure 7. A total of 32 data acquisitions were made during the experiment, resulting in an acquisition frequency of approximately 2 hr. The results of the time-lapse survey were able to map the evolution of saturation within the slope, as well as determine the bedrock geometry of the area under investigation. The authors recommended increased acquisition rates during the experiment to better monitor wetting processes, and the incorporation of 3-D arrays to improve the quantitative analysis of the data, primarily due to the suspected 3-D effects that are likely to have occurred during the experiment, but that are not captured by the 2-D inversion approach of the data.

The study by Travelletti et al. (2012) showed a relatively high frequency of data acquisition over a short period of time, and in this regard is similar to other artificial rainfall experiments which utilized time-lapse ER methods (Grandjean et al., 2009; Jomard et al., 2007; Lehmann et al., 2013). The time scales and acquisition rates of these studies are in contrast to longer-term studies that utilize transient measurements and semipermanent installations. In one study by Bièvre et al. (2012), transient time-lapse ER measurements were used to determine the role of fissuring on water infiltration over a 498-day period, by acquiring four time-lapse ER data sets in the unstable clay slopes of the Avignonet landslide in the Trièves area of the French Alps, France. Although the campaign lasted over a year, resistivity data sets were acquired at 0, 29, 236, and 498 days, showing an irregular acquisition schedule. Despite the relatively low-frequency and irregularity of acquisition, the time-lapse approach suggests that the observed evolution of fissuring shows variations in resistivity that are related to the water storage capacity of the fissures. Higher-frequency data set acquisition would benefit the monitoring of the evolution of fissure-aided infiltration.

The use of semipermanent 3-D arrays and regular acquisition schedules are able to overcome the issues of irregular acquisition rates and 3-D effects in 2-D surveys, and pseudo-3-D surveys interpolated from 2-D data sets. These 3-D effects occur where a feature which may not be directly located beneath the ER profile influences the data. Such a study was described by Uhlemann et al. (2017), in which a semipermanent time-lapse monitoring system was used to collect 3-D ER data approximately every two days at the Hollin Hill landslide in North Yorkshire, UK. The study

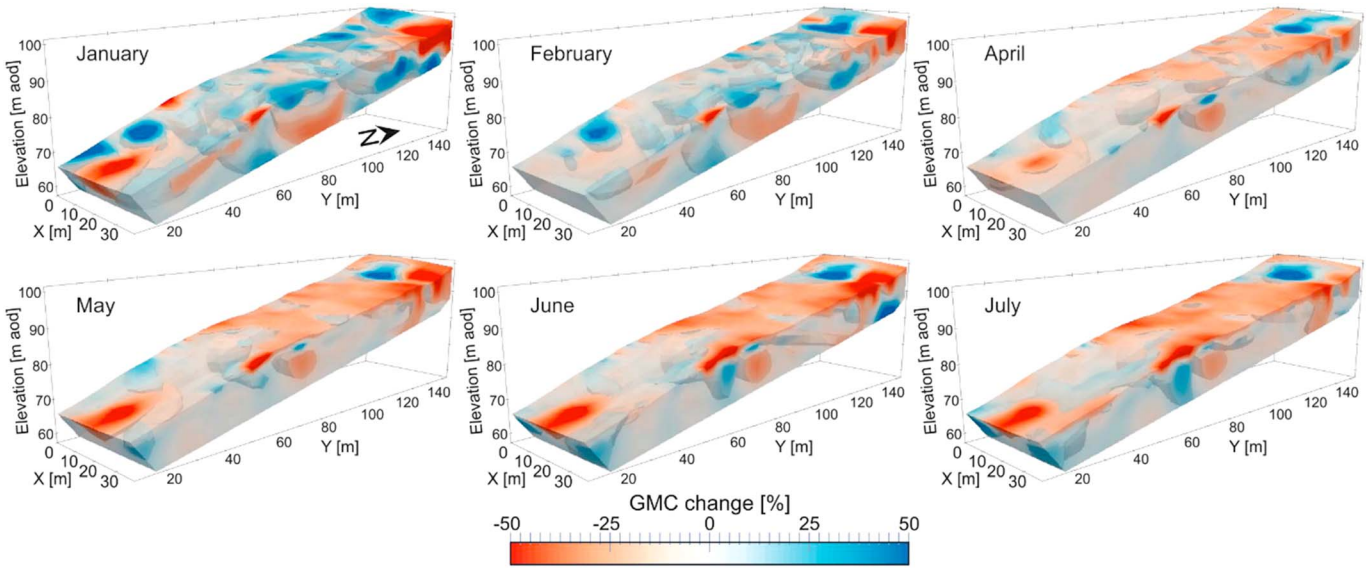

Figure 8. Volumetric images of gravimetric moisture content (GMC) derived from a 3-D time-lapse ER system (Uhlemann et al., 2017) showing the progressive drainage of a landslide after significant movement in December 2012. Volumetric images shown here are from the later part of a monitoring campaign spanning over three years, and show the changes in GMC relative to a baseline model acquired at the beginning of the monitoring period in March 2010. Modified from Uhlemann et al. (2017). Copyright © 2017 by John Wiley & Sons, Inc. Reprinted by permission of John Wiley & Sons, Inc.

involved several other novel aspects beyond the incorporation of 3-D data acquisition. First, inversion models were able to account for movement experienced by the electrodes in the sliding mass (Wilkinson et al., 2016), which can introduce significant errors in the data if not accounted for. Additionally, the resistivity data were converted to gravimetric moisture content (GMC) by fitting of a Waxman-Smits model (Waxman & Smits, 1968) to laboratory experiments of wetting and drying of samples obtained from the site (Merritt et al., 2016). This allowed the production of volumetric images of GMC data, showing the hydrogeological variation in the landslide body both before and after a slope failure in December 2012 (Figure 8).

Other long term time-lapse ER studies have utilized data in other novel ways in order to capture subsurface moisture variations within landslides over time. Studies utilizing noninverted ER data as an indicator of hydrological variation have been made by several authors. These studies were able to detect features such as water table variations (Palis, Lebourg, Tric, et al., 2017), links between hydrological patterns and changes in apparent resistivity (Lebourg et al., 2010; Palis, Lebourg, Vidal, et al., 2017), and relationships between resistance data and subsurface moisture dynamics (Merritt et al., 2018). In each of these studies, the data required significantly less processing than if tomographic inversion of the data had taken place.

After conducting time-lapse surveys to confirm the application of ER to the Vence landslide in south-eastern France, Lebourg et al. (2010) used apparent resistivity correlations compared to rainfall and groundwater levels to conduct multidimensional statistical analysis and determine prerainfall and postrainfall states of the landslide over a 90-day monitoring period. The simultaneous presentation of individual apparent resistivity measurements alongside rainfall events over a 275-day monitoring period at a landslide at Ampflwang-Hausruck, Austria, by Supper et al. (2014) allowed for rapid observations of the response of measurements to rainfall events to be made without the need for time-lapse inversions. However, it is worth noting that Supper et al. (2014) still produced time-lapse inversions for detailed determinations of movement events and relationships with precipitation. At the La Clapière landslide in the Alpes Maritimes, France, Palis, Lebourg, Vidal, et al. (2017) compared the median apparent resistivity value from a semipermanent ER system to a cumulative rainfall index, and observed both short-term decreases in resistivity associated with acute rainfall events, as well as longer seasonal variability linked to solar radiation. Apparent resistivity data from a 9.5-year monitoring period was statistically analyzed using cluster analysis in a study by Palis, Lebourg, Tric, et al. (2017). The results of the study allowed the determination of distinct hydrogeological units within the landslide without the need to make assumptions about the local geology, identifying areas of the landslide that react differently to water infiltration. However, the authors ultimately recommend further work to

establish petrophysical relationships between the resistivity and moisture content, similar to the approaches undertaken by Uhlemann et al. (2017). Merritt et al. (2018) utilized resistance measurements to conduct rapid observations of moisture dynamics at the Hollin Hill landslide in North Yorkshire, UK. The resistance data were derived from the same ER system used in the study by Uhlemann et al. (2017). As resistance data can be analyzed before the process of inversion, the study proved to be a rapid means of assessing the near surface of the Hollin Hill landslide to identify areas of potential preferential infiltration. This type of approach can prove useful for the determining areas of a landslide in which more computationally expensive investigations should be undertaken.

4.4.2. Passive Geoelectrical Methods

4.4.2.1. SP

Self-potential (SP) techniques measure the presence of naturally occurring charges in the Earth surface, primarily streaming potentials and electrochemical potentials, although thermokinetic potentials and cultural activity may also be recorded (Colangelo et al., 2006). As such, SP is defined as a passive geophysical method. Potentials between pairs of electrodes are measured to create areal maps of variation in self-potentials. In the context of landslides, this is normally to determine areas of subsurface flow within the subsurface material. As with electrical resistivity, semipermanent arrays of electrodes can be installed to facilitate high-frequency, long-term monitoring campaigns. Tomographic inversion of 2-D and 3-D surveys can be undertaken to ascertain information in cross section and volumes (Ozaki et al., 2014).

Only one study used SP monitoring of landslides (Colangelo et al., 2006) in which temporal fluctuations of SP signals were monitored over a 24-hr period during a period of precipitation. A linear array of electrodes were deployed, and the data were inverted (to produce a tomographic inversion cross section) to show the dynamics of subsurface flow during the rainfall event. The study describes in a qualitative manner the variation in flow, instead of moisture content as normally targeted by ER surveys. As the SP method does not give any information in itself on geological characterization, the interpretations were made with the knowledge acquired from previous SP mapping and ER investigations of the landslide setting.

4.5. Seismic Monitoring Case Studies

As with geoelectrical methods, seismic methods can be split between active and passive methods. Active seismic monitoring records seismic signals generated by artificially produced sources. Passive methods tend to record seismic signals either generated by endogenous landslide activity (i.e., seismic signal produced by landslide movement) or analyze ambient signals from exogenous sources.

4.5.1. Active Seismic Methods

Active seismic methods provide information about the elastic properties of the media through which seismic waves travel. This reveals geomechanical properties of subsurface materials and can indicate changes in the subsurface stress conditions associated with movement, as well as providing information on the porosity of materials, and in turn fluid flow characteristics.

Seismic refraction (SR) and surface wave methods (SW) use field deployments of surface geophones linked to a seismograph to record properties of artificially generated seismic waves. In SR, the arrival times of compressional waves (*P* waves) and shear waves (*S* waves) are recorded. *P* and *S* waves are typically generated using an impact source (e.g., a sledgehammer). *P* waves are generated by a vertical impact to a plate resting on the ground surface, and recorded using geophones sensitive to movement in the vertical direction. *S* waves are generated by a horizontal impact to a plate coupled to the ground, and the resultant waves recorded by geophones sensitive to motion in the horizontal plane. The arrival times ("first breaks") on each geophone give information about the refracted pathway taken by the wave between the source and geophone. This information can then be inverted to give a model of the *P* wave or *S* wave distribution in the subsurface, which can then be interpreted in terms of variations in elastic properties of the subsurface.

SW methods record surface waves (primarily Rayleigh waves, although Love waves can also be analyzed), which are typically much slower and of greater amplitude than refracted *P* waves and *S* waves. Analyzing the frequency content of these waves can be used to produce dispersion curves, which show phase velocity as a function of frequency. By analyzing the fundamental mode energy in these images, a surface-wave velocity inversion is used to produce a 1-D model of *S* wave velocity as a function of depth. Lateral measurements of surface-wave velocity profiles can then be collated to produce 2-D sections of interpolated *S* wave velocity throughout the ground. Calculating *S* wave velocity from surface waves is

often preferred by investigators, as the field setup for acquiring surface waves is effectively the same as that of a *P* wave SR survey, removing the need to repeat *S* wave SR surveys to obtain *S* wave velocities (Bergamo et al., 2016; Pasquet et al., 2015).

Two case studies utilized active seismic monitoring methods in landslide settings. Of these, one used SR surveys (Grandjean et al., 2009) and one utilized SW methods (Bièvre et al., 2012). Both studies achieved the stated aims of the experiments, but show relatively poor potential for obtaining long-term data sets at frequent intervals; indeed, no examples of semipermanent installations of active source SR or SW applied to landslides are apparent in the literature. This is likely due to the relative complexity of remotely generating the necessary seismic sources, although analogous borehole systems do exist (Daley et al., 2007).

4.5.1.1. SR

In the study of Grandjean et al. (2009), the main focus of the time-lapse *P* wave SR surveys was to determine fissure density during a simulated rainfall experiment on a landslide in the Laval catchment in Alpes-de-Haute Provence, France. The *P* wave survey was undertaken using a 48-channel seismic system, using 40-Hz geophones and a hammer source. The aim of the survey was to integrate the SR data sets with simultaneously collected ER data sets using a fuzzy logic approach. Direct analysis of the *P* wave SR suggested that low *P* wave velocities in the near surface were due to increased fissure density. However, in contrast with the ER survey, *P* wave SR showed very little change with increasing saturation over the course of the experiment, which underscores the usefulness of integrated use of SR and ER surveys.

4.5.1.2. Analysis of SW

Bièvre et al. (2012) used the variations in SW dispersion (Rayleigh waves) to assess the state of fissuring in the clay-rich slopes of the Avignonet landslide in the Trièves area of the French Alps, France. Surface waves were acquired using 24 4.5-Hz geophones, and a hammer source. Analyses of the surface waves using amplitudes and spectral ratios were undertaken for two different acquisition dates, one in January and the other in July, in order to determine relative differences between the states of fissuring on each occasion. The authors determined that the fissures remained open at these different times, with some possible minor variation in the depth of the fissures.

4.5.2. Passive Seismic Methods

In order to obtain continuous seismic data over longer monitoring periods, it is necessary to look to methods more typically adopted by the seismological monitoring community for the assessment of large-scale natural hazards such as volcanoes and earthquakes (Daskalakis et al., 2016). In recent years, the application of passive seismic monitoring techniques have increasingly been applied to engineering issues (Öz, 2015), with notable advances in the field of ambient noise measurements and the application of spectral analyses to passive measurements (Park & Miller, 2008; Planès et al., 2016). Early work by Suriñach et al. (2005) identified changes in the frequency content of seismic records at avalanche and landslide sites that were associated with initiation of mass movement.

Although the treatment and processing of passive seismic data vary depending on the intended use, the principal style of acquisition is essentially the same. A seismic recording instrument is left for a period of time to record signals that may be generated by movement within the landslide body, or signals that are generated by known or unknown, endogenous and exogenous sources. The instruments used can be geophones (typically for shorter recording periods), broadband seismometers, or other adapted sensors (e.g., accelerometers). Properly maintained and adequately powered semipermanent installations of seismic sensors are able to record continuous data sets for very long time scales. For example, the monitoring period in a study by Renalier, Jongmans, et al. (2010) exceeded 2.5 years. Some studies employ sensor deployments for much shorter periods of time (i.e., $<$100 days; e.g., Amitrano et al., 2007), in what have been described here as short-term installations. These deployments are generally short due to equipment availability or the lack of in-field power sources to maintain long monitoring periods. Single-sensor deployments can be used, for example, to detect movements within an area (e.g., Amitrano et al., 2007), or multiple-sensor deployments can be used for more detailed interpretations (e.g., Brückl et al., 2013).

The case studies reveal a range of data analysis methods using passive seismic approaches. To simplify the description of approaches, the use of passive seismic methods is split into four categories: seismic horizontal-to-vertical ratio measurements (S-H/V), event detection, characterization and location (S-EDCL), seismic ambient noise cross-correlation (S-CC), and seismic ambient noise tomography (S-ANT).

4.5.2.1. S-H/V

The S-H/V technique involves recording ambient noise and analyzing the Fourier amplitude spectra ratio between the horizontal and vertical components of the seismometer, known as the horizontal-to-vertical ratio (Chatelain, 2004; Nakamura, 1989). The resulting S-H/V spectral ratio curves can be used to determine relative seismic impedance in the subsurface, and can therefore identify changes in layer thicknesses or the presence of other features, such as slip planes.

S-H/V methods have been used in two studies to monitor landslides (see Appendix A), but with two very different approaches. In Amitrano et al. (2007), S-H/V measurements were made from a short-term installation of a single broadband seismometer located at the Super-Sauze landslide in France. The calculated cumulative RMS of the S-H/V ratio for several frequency bands showed a correlation with periods of increased rainfall, indicating changes in the mechanical properties of sliding material during periods of acceleration.

Imposa et al. (2017) utilized a transient measurement approach, using a sensor specifically designed for the acquisition of S-H/V readings. These readings were acquired at the same stations in two separate surveys separated by five years. For transient S-H/V measurements, recording durations between 2 and 24 min are typically used (Acerra et al., 2002). The individual S-H/V spectral ratios that are produced per sensor location were processed and interpolated to produce cross sections of seismic impedance, showing changes in the location of the potential slip surface postfailure.

4.5.2.2. S-EDCL

S-EDCL utilizes the more traditional aspects of seismology commonly applied in earthquake and volcano monitoring. The approach is to detect events and classify them based on the source provenance and generation. This approach involves direct interpretation of the signals recorded by semipermanent seismic sensors, either by identifying and classifying seismic events associated with movement in the landslide mass (i.e., "slidequakes" (Gomberg et al., 1995)) or by precursory activity that may be linked to impending movement (a phenomenon observed in rockfalls and other brittle landslides (e.g., Bell, 2018, Poli, 2017)), or a response to recent increased infiltration (e.g., Palis, Lebourg, Vidal, et al., 2017). A single seismic sensor installation is capable of achieving this type of monitoring (e.g., Amitrano et al., 2007); however, a network of seismometers is required to locate detected events (e.g., Walter et al., 2011). It is worth mentioning here that S-EDCL methods are also the only approaches used in the near-real-time detection and characterization of landslides at the regional scale (e.g., Kao et al., 2012; Manconi et al., 2016), and are commonly used in studies relating to rockfalls and other fast-failing landslides.

An example of event detection and characterization is described in Provost et al. (2017). In this study, the authors proposed an automatic classification system, in order to identify and separate seismic events recorded at the Super-Sauze landslide in France based on their source and provenance. Sources included signals from rockfalls and slidequake events within the landslide, and earthquakes and ambient noise events originating from outside the landslide setting. Example seismic signals are shown in Figure 9.

Brückl et al. (2013) undertook seismic monitoring of the Gradenbach landslide in Austria. They were able to locate events recorded using six seismometers installed at the site, and noted increases in seismic activity up to 1.5 months before the manifestations of slope deformations which coincided with snowmelt. Palis, Lebourg, Vidal, et al. (2017) also noted increased seismic activity as a result of increased precipitation at the La Clapière landslide, France, aiding in the establishment of rainfall threshold values for slope movement at the site.

The studies by Gomberg et al. (2011) at the Slumgullion landslide in the United States, Walter et al. (2011) at the Heumoes landslide in Austria, and Walter et al. (2012) at the Super-Sauze landslide in France are all summarized in a study by Walter et al. (2013). The authors related increases in seismic activity to brittle failure (i.e., fracture generation) of the landslide material, but also noted periods of movement that were not associated with increases in seismic activity. These aseismic movement events were related to periods of viscous creep, rather than brittle failure events. Location of the seismic sources of these events showed very different areas of seismic activity, and a strong association with the profile of the slip surface, the type of materials present, and the style of failure. Figure 10 shows the slidequake events located at the Heumoes landslide using S-EDCL methods (Walter et al., 2013).

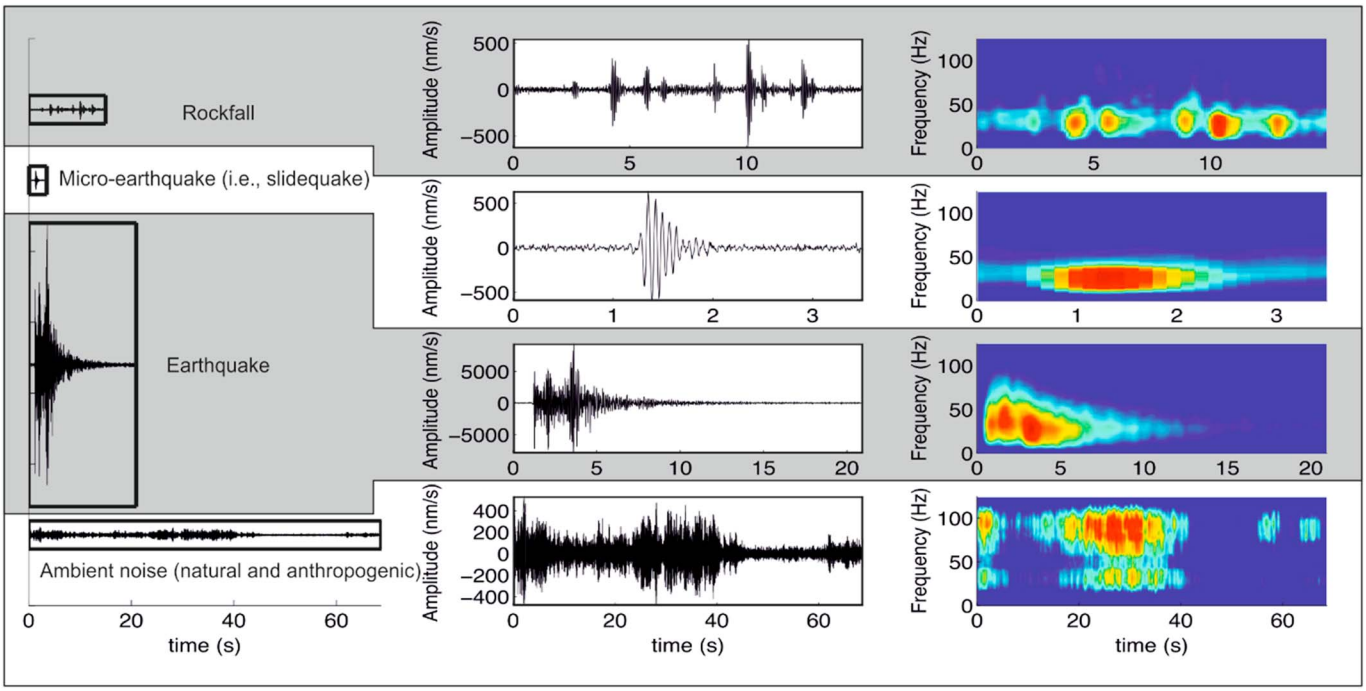

Figure 9. Example of seismic event detection and classification at the Super-Sauze landslide. The types of seismic events include endogenous (rockfall and slidequake) and exogenous (earthquake and ambient noise) events. Modified from Provost et al. (2017). Copyright © 2017 by John Wiley & Sons, Inc. Reprinted by permission of John Wiley & Sons, Inc.

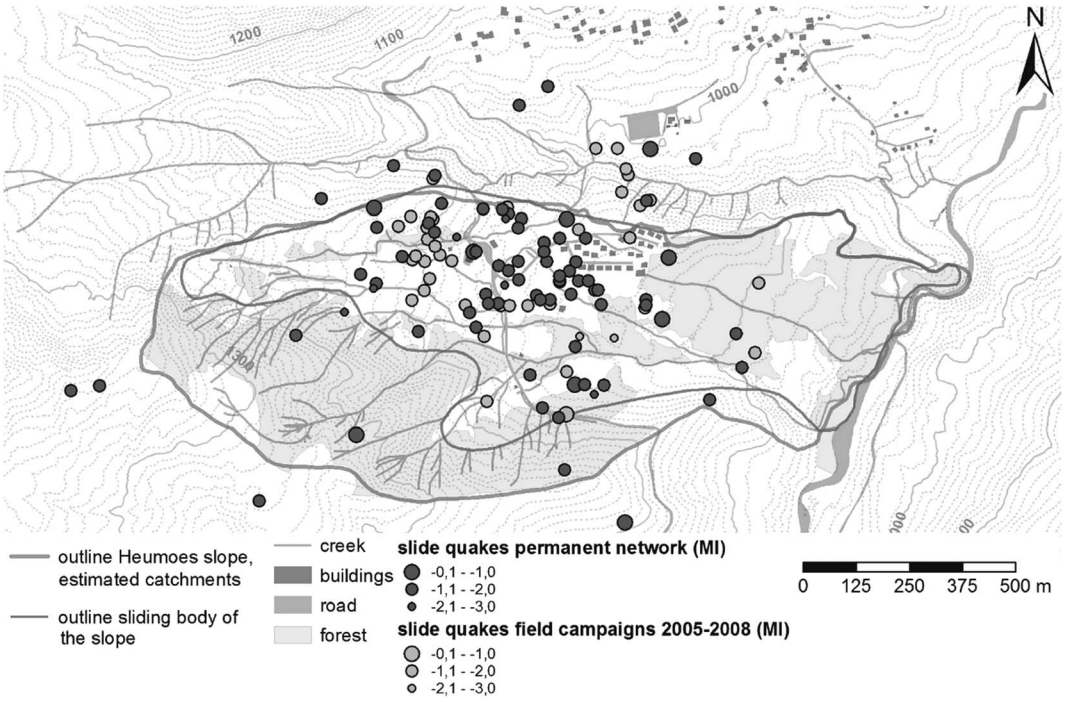

Figure 10. Locations and magnitudes of slidequake (i.e., seismic activity generated by slope movement) events detected at the Heumoes landslide, Austria, by several seismic networks. Events are identified by different size and color dots on the map. The seismic networks include one semipermanent installation (see "permanent network") and several short-term deployments (see "field campaigns 2005–2008"). From Walter et al. (2013). Copyright © 2013 by Environmental and Engineering Geophysical Society. Reprinted by permission of Environmental and Engineering Geophysical Society.

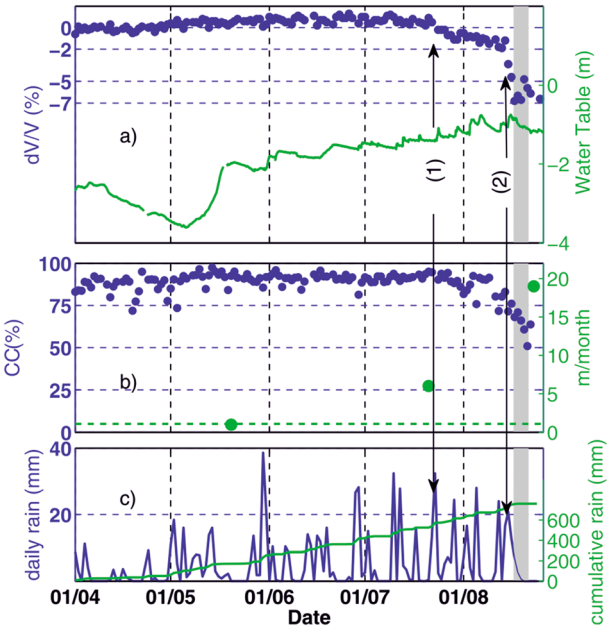

Figure 11. (a) The results from calculating changes in relative surface-wave velocity over time via cross correlation of ambient noise seismic records by Mainsant et al. (2012). Decreases in velocity by 2% develop over 20 days (1), before a total decrease of 7% is observed (2) in the seven days preceding a significant failure (shaded gray area). (b) The cross-correlation coefficient and (c) the daily and cumulative rainfall. From Mainsant et al. (2012).

4.5.2.3. S-CC

Cross-correlating signals from a pair of seismic sensors recording the same random ambient noise can be used to generate the impulse signature (Green's function) of wave propagation between sensors (Wapenaar et al., 2010). Many sources of natural and anthropogenic noise can be utilized (for example, oceanic noise, vehicle traffic noise) if the source can be averaged over time to simulate a random ambient source. These cross-correlation functions (CCFs) can be used to monitor variations in surface-wave velocity over time, indicating changes in the stress field of subsurface materials (Lecocq et al., 2014).

Two of the case studies (Appendix A) utilize cross-correlation methods to determine variations in geological material strength over time within moving landslides. Renalier, Jongmans, et al. (2010) observed increases in seismic wave arrival times between two semipermanent seismometers over a 32-month monitoring period at the Avignonet landslide in the Trièves area of the French Alps, France. The differential in arrival times equated to an almost 0.2% decrease in velocity over time, with relative differences in ground motion between the seismometers only able to account for an equivalent of a 0.06% change in seismic wave arrival times. The authors concluded that the increase in arrival times corresponded to an increase in "damage" (i.e., fissuring and destruction of soil fabrics) to the material of the landslide. This area of damaged material was characterized by a stand-alone *S* wave SR survey, in which the velocity of the damaged material was shown to be 2 to 3 times less than the surrounding undamaged area.

A study by Mainsant et al. (2012) over a shorter period of 146 days at the Pont Bourquin landslide in Switzerland was able to detect variation in surface-wave velocities a few days before significant slope failure on 19 August (Figure 11). A drop of 2% in surface-wave velocity occurred over a period of 20 days after heavy rainfall, with the surface-wave velocity dropping a further 5% in the seven days preceding a significant failure at the landslide. The study highlights the applicability of long-term seismic monitoring to determining variations in subsurface material strength, and also the potential landslide predictive capacity of seismic monitoring.

4.5.2.4. S-ANT

A frequency-time analysis of the outputs from cross correlations can allow for the generation of dispersion curves (Bensen et al., 2007), which can in turn be inverted for the *S* wave velocity of the near surface (e.g., Stork et al., 2018). Interpolation of the inverted dispersion curves between sensor pairs allows for the production of images similar to those seen in previous active seismic and geoelectrical techniques. Linear deployments of sensors allow the acquisition of data in 2-D profiles, and studies have been able to image landslide bodies in 3-D using nonlinear arrays, although these have not incorporated a time-lapse element yet (Renalier, Bievre, et al., 2010).

Only one case study produced these cross-section images by acquiring transient measurements on separate dates acquired from an array of 12 seismometers. In the study by Harba and Pilecki (2017), ambient noise data were acquired for 60-min periods at two profiles using 12 seismometers. Measurements were made at the profiles at three separate dates over seven months. The study took place at the Just-Tegborze landslide in Nowy Sacz, southern Poland. The first acquisitions were made during a dry period in January 2015, the second acquisitions in March 2015 after the spring thaw, and finally during a very wet period in July 2015. The 1-D inversions of dispersion curves were performed on the cross-correlated signals between sensor pairs, and the subsequent interpolated 2-D cross sections showed variations in the shear-wave velocity distribution throughout the landslide mass between acquisition dates (Figure 12). The authors attribute the decreasing shear-wave velocity in the midsection of the landslide to the increasing moisture content of the landslide associated with spring thaws and increased rainfall.

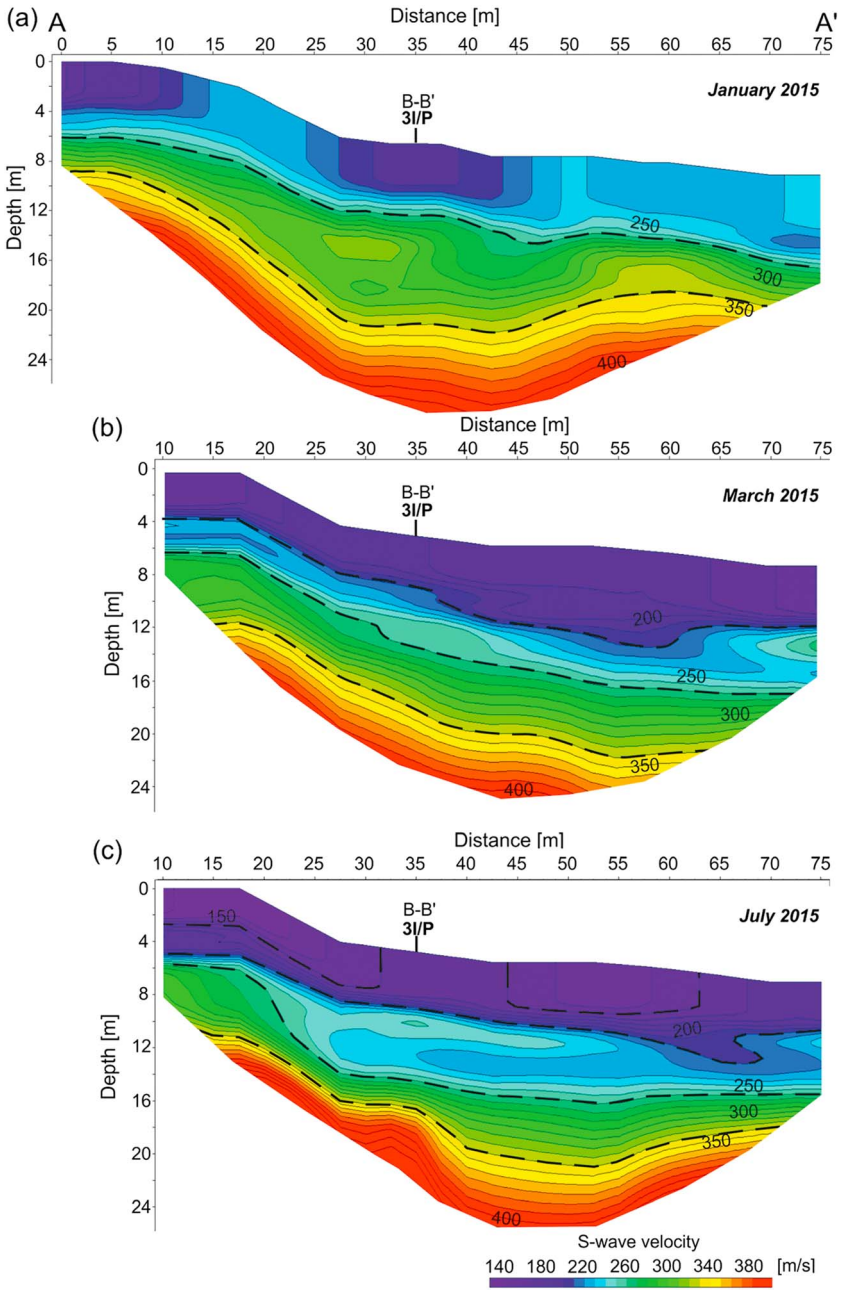

Figure 12. The results of ambient noise tomography (ANT) undertaken on a series of transient measurements acquired from seismometers by Harba and Pilecki (2017). Ground moisture is increasing from January to July, likely causing the observed in decrease shear-wave velocity in the landslide body. From Harba and Pilecki (2017). Copyright © 2016 by John Wiley & Sons, Inc. Reprinted by permission of John Wiley & Sons, Inc.

4.6. Integrated Surveys

The preceding section has focused on the individual methods utilized for the geophysical monitoring of landslides. One major limitation of geophysical investigations is the nonuniqueness of results obtained from surveys. The process of data inversion reduces this inherent ambiguity by providing spatial distributions of geophysical parameters. However, inversion of geophysical data is in itself a nonunique problem, as usually an infinite number of subsurface models can explain the data equally well and constraints need to be introduced to obtain the most likely subsurface distribution of the sought parameter. Although this nonuniqueness of both raw and inverted data can be addressed, one major limitation remains that an individual

method is normally only sensitive to one physical property in the subsurface, the distributions of which may be variable in both time and space, and the occurrence of which may depend on several transient factors.

4.6.1. Multiparametric Geophysical Monitoring

Multiple methods can reduce the uncertainty in the assumptions made about the ground condition by comparing the interpretations of each. Further quantitative analysis can be made by the use of joint inversions which incorporate physically constrained factors when creating models of the ground condition. This approach is referred to here as "multiparametric geophysical monitoring."

Relatively few examples are present in Appendix A, in which more than one geophysical method has been utilized in a monitoring campaign. Multiparametric geophysical monitoring campaigns (i.e., utilizing more than one acquisition method) have been used in three of the studies identified in Appendix A, with all using ER and SR methods (Bièvre et al., 2012; Grandjean et al., 2009; Palis, Lebourg, Vidal, et al., 2017).

In the study by Grandjean et al. (2009), ER and SR surveys were carried out on co-located survey profiles across the Laval landslide in Draix, south French Alps. The results of the two independent surveys were fused using a fuzzy logical approach, utilizing probabilistic methods to test the validity of expert hydrological meta-hypotheses across the area of the monitored subsurface. This approach allowed for the independent results of each method to be combined during a controlled rainfall experiment, resulting in the quantification of the development of expected phenomena (e.g., presence of fissures, development of saturated zones, and areas of high porosity). This study is the most in-depth attempt to fuse data in such a way that the output of the study is more robust than the typical cross sections of property distributions normally found in geophysical surveys. The probabilistic approach of the study also pays significant attention to the reliability, or conversely the uncertainty, of the data, another area that can be overlooked in the application of geophysical methods.

In the studies by Bièvre et al. (2012) and Palis, Lebourg, Vidal, et al. (2017), the geophysical data sets are not interpreted in such a joined quantitative manner, but instead, all contribute to the overall qualitative interpretation of the landslide processes at play in the individual studies. For example, Bièvre et al. (2012) exploited the sensitivity of electrical resistivity methods to the presence of water-infiltrating fissures, and the effect of attenuation on surface waves caused by the presence of fissures to determine extents of fissuring in the near surface of the clay-rich Avignonet landslide. The different properties assessed by the two techniques were able to qualitatively confirm the hypothesis that fissuring played an important role in the infiltration of water at the landslide, despite the independent acquisition and processing of the data sets. Similarly, Palis, Lebourg, Vidal, et al. (2017) were able to link changes in the annual climatic cycle to variations in seismic monitoring responses and electrical resistivity values, allowing for a better understanding of the response of the landslide processes to external influences such as increased rainfall.

4.6.2. Environmentally Coupled Monitoring

Incorporation of environmental data (e.g., rainfall data, displacement rates) allows for the temporal variations in geophysical monitoring data to be classified as being due to causative property changes in the landslide (e.g., increased saturation preceding failure) or resultant property changes (e.g., seismic responses generated by movement of the landslide). Incorporation of these external data sources is referred to in this review as "environmentally coupled geophysical monitoring." The importance of monitoring environmental fluctuations has been noted by several authors. Luongo et al. (2012) stated the importance of a weather monitoring station at the location of a prototype semipermanent ER system, and similar local weather data were collected in other studies (Uhlemann et al., 2017). Particularly with ER, external environmental variations, most notably thermal variations, have a strong influence on the data, and thermal effects need to be corrected (Lucas et al., 2017).

The displacement of landslides does, however, present a problem for ongoing monitoring using geophysical methods. As mentioned previously, the success of monitoring campaigns depends on being able to accurately spatially locate the datum at which measurements are being taken. In some types of geophysical monitoring approach, for example, when using single-seismometer monitoring for event detection, the detailed location of the seismometer and its movement over time may not be of consequence to the aim of the monitoring (Amitrano et al., 2007). However, in some other methods, such as semipermanent installations of ER arrays, movements in electrodes can have profound effects on the data quality, creating artifacts in the data if unaccounted for. This is typically overcome by periodic measurement of the movement of electrodes. These positional measurements need to be taken at a frequency at which movement can be captured.

Recent advances in geophysical inversion have been able to recover electrode movements over time, and therefore incorporate the movements in to the processing of ER data to prevent the introduction of data artifacts by electrode movements (Boyle et al., 2017; Loke et al., 2017; Wilkinson et al., 2010; Wilkinson et al., 2015). This has been an important step in developing the autonomy of semipermanent installations, and has greatly improved the data quality available from such campaigns (Uhlemann et al., 2017).

Establishing thresholds for landslide movement from geophysical data coupled with environmental data is a critical component of understanding subsurface process evolution. Palis, Lebourg, Vidal, et al. (2017) were able to establish a rainfall threshold of 3.5 ± 1 mm/day above which the seismic sensors at the La Clapière recorded increased endogenous events associated with movement. Palis, Lebourg, Vidal, et al. (2017) also showed that long-term analysis of rainfall with ER and S-EDCL methods allowed for the variable kinematics of the landslide to be established, with the authors noting delayed responses in displacement rates associated with the intensities, durations, and repeat intervals of rainfall events. In many cases however, the determination of thresholds from rainfall alone coupled to geophysical responses is unlikely to be successful unless the infiltration rate is well understood, as the subsurface moisture dynamics that can vary greatly depending on lithology, precipitation, temperature, etc., are not captured by such a simplified relationship. This is particularly apparent where effective rainfall (i.e., the amount of water that arrives at ground level, which is not inhibited by evapotranspiration) or effective infiltration (i.e., the amount of water reaching the subsurface, which is not inhibited by evapotranspiration and surface runoff) is not taken into account. A further approach can therefore be to couple geophysical responses to monitoring measurements made from the subsurface, via the use of geotechnical monitoring methods.

4.6.3. Geotechnically Coupled Monitoring

Even with the incorporation of multiple geophysical methods to landslide monitoring, the sensitivity of the geophysical method (or methods) is to the changes in the soil or rock property that is being monitored, rather than being a direct measurement of the property itself. For example, shear-wave velocity can be used to calculate shear strength of the subsurface when other data (i.e., density data) are incorporated, but it is not a direct measurement of shear strength. In order for geophysical measurements to be of use to end-users (who may not be geophysicists), the results need to be coupled to known parameters in the landslide environment. The relationship between geophysical measurements and the petrophysical properties of rocks and soils has most widely been applied in the hydrocarbon exploration industry (Barton, 2007). These coupling relationships are normally established by the careful selection and preparation of representative samples of subsurface material, upon which laboratory tests to determine the relationship between environmental influences (e.g., soil moisture), petrophysical properties (e.g., porosity, density), and a geophysical response (e.g., electrical resistance) can be established, as in the example of Merritt et al. (2016). A study by Carrière et al. (2018) into the rheological properties of soil samples from six clay-rich landslides across Europe recommended the application of geophysical methods for determining the properties of slide-to-flow dynamics. The main challenge to establishing reliable geophysical-petrophysical relationships is that of sample selection, and ensuring that samples collected and tested are representative of the conditions of subsurface materials, as landslides typically have highly heterogeneous subsurface conditions (van Westen et al., 2006).

Upon the establishment of such relationships the ability to then compare the results of these geophysical-petrophysical relationships with data gathered from sensors installed in landslides is referred to here as "geotechnically coupled monitoring." Lehmann et al. (2013) determined the relationship between soil moisture as measured by time domain reflectometer sensors at the same time as ER measurements during two simulated rainfall tests. From this relationship they were able to produce cross sections of volumetric moisture content (VMC) and demonstrate the variations in VMC over time. In a study by Lucas et al. (2017), VMC was measured directly by several sensors on site, and the data used to derive a relationship between ER measurements and VMC, allowing for reliable spatial subsurface mapping of VMC. The authors noted the benefit of using ER for determining VMC values at a large spatial resolution, but noted the need for care in calibrating the ER measurements to determine VMC. In a similar study, Travelletti et al. (2012) were unable to establish a relationship between moisture content and ER data due to issues with nonuniqueness in the ER data, and scalability issues with using sparsely located moisture content measurements derived from point sensors. This issue of inherent heterogeneity and extrapolation of data from a sparse network of direct measurement sensor remains a challenge for geotechnically coupled geophysical monitoring.

Uhlemann et al. (2017) established a relationship between ER values and laboratory determined values of gravimetric moisture content (GMC) from samples collected at the landslide site rather than using measurements derived from sensors during the geophysical monitoring period, although retrospective comparison between the ER-derived GMC and sensor-measured GMC was in good agreement. The authors were then able to establish a failure threshold based on GMC, rather than rainfall, a measurement that better reflects the complex interactions between rainfall and subsurface moisture. In particular, estimated values of subsurface moisture content have implications for soil suction, which can be one of the most important stabilizing forces in landslides (Toll et al., 2011).

The complexities of establishing such relationships in practice are identified by Hen-Jones et al. (2017), who identified that such geotechnically coupled relationships often display hysteretic behavior in relation to seasonal variations, adding a temporal heterogeneity to the already present spatial heterogeneity present in landslide settings. An additional consideration is that, in a similar way that geophysical responses can be caused by a multitude of factors, geotechnical property variations can have a variety of causes, for example, the reduction of shear strength in soils due to loss of suction in wetting and drying cycles, and soil fabric deterioration across successive seasonal cycles (Hen-Jones et al., 2017).

5. Discussion

5.1. Strengths in Geophysical Monitoring of Moisture-Induced Landslides

There are three areas in which the geophysical monitoring of landslides are particularly successful. These are the following:

1. Providing high-resolution spatial information on landslide features (i.e., discrete spatial features).
2. Providing high-resolution temporal information on the evolution of landslide processes (i.e., analyzing how a subsurface property has changed over time and inferring the causal process).
3. Calibrating and coupling data with other sources of environmental and geotechnical information.

The first area, the provision of high-resolution spatial information on landslide setting features, is an extension of the aforementioned benefits of geophysical methods in earlier sections (Jongmans & Garambois, 2007; Mccann & Forster, 1990). The same advances in technology that have allowed for the establishment of permanent monitoring installations have also allowed for greater measurement accuracy and resolution (Loke et al., 2013). The application of geophysical methods to image the subsurface between direct measurement locations is well established (Parsekian et al., 2015), and typically is where the use of near-surface geophysical methods lends most benefit to ground investigations. This can allow identification of features including the slip surface (Harba & Pilecki, 2017), analysis of the volumetric extent of disturbed materials (Uhlemann et al., 2017), and identification of deformation features and preferential infiltration pathways (Bièvre et al., 2012). Images, produced by tomographic inversion of data, can be assessed by comparative image analysis (e.g., Friedel et al., 2006), or through difference analysis compared to an initial image (e.g., Lucas et al., 2017). Direct measurements from these sources is near essential in the accurate interpretation of geophysical images, highlighting the complementarity between well-sited direct measurements (the placing of which can be optimized by geophysical methods) and geophysical images of the subsurface. The geophysical images produced are further enhanced by the expansion from 2-D to 3-D data capture (Uhlemann et al., 2017) and relation to property distributions (Crawford & Bryson, 2018; Lehmann et al., 2013).

The second area of strength for monitoring relates to the progression of landslide processes. These processes include rapid moisture infiltration in response to acute rainfall (Travelletti et al., 2012), seasonal variations in subsurface moisture content (Uhlemann et al., 2017), short-term variations in ground saturation (Lehmann et al., 2013) and material strength (Mainsant et al., 2012) immediately preceding failure, measurements of flow in landslide bodies (Colangelo et al., 2006), and detection of landslide movement (Brückl et al., 2013). The temporal resolution of data that can be obtained from geophysical monitoring campaigns in many cases can match those of installed point sensors (i.e., daily or subdaily measurements), while in many cases still producing subsurface images that cannot be obtained from such sensor networks (Supper et al., 2014).

The third area is the one in which most development is required, but perhaps the area in which the most stands to be gained for monitoring of landslides. Demonstrated data-coupling approaches include linking changes in geophysical measurements to rainfall (Palis, Lebourg, Vidal, et al., 2017) and ground moisture

(Uhlemann et al., 2017) thresholds preceding failure, establishing property relationships between volumetric moisture content and ER measurements (Lehmann et al., 2013; Lucas et al., 2017) and shear strength parameters and ER measurements (Crawford & Bryson, 2018). It is in this area that geophysical monitoring approaches can contribute most to slope-scale EWS, not only due to the spatial and temporal resolution of data but by linking these data to other areas of landslide study that can be understood by the wide range of stakeholders involved in the establishment, maintenance, and management of EWS.

S-EDCL approaches are well represented in the literature, but currently deal primarily with a retrospective analysis of seismic signals generated by landslides failure. ER monitoring is particularly well suited to monitoring precursory infiltration and subsurface movements and distributions of water, which is a key driver in the destabilization of landslides through the reduction of matric suctions in partially saturated conditions (Toll et al., 2011). In addition to this, the application of ER monitoring has seen large interest not only in the field of landslide investigation and monitoring (Perrone et al., 2014) but also in other areas of hydrogeophysical research (Binley et al., 2015). This interest has driven technological advancements in the application of geoelectrical monitoring of landslides, something which is likely reflected in the increasing length of monitoring periods and frequency of data set acquisition over time. A geotechnically coupled approach is important in informing the predictive capacity of geoelectrical monitoring systems. When integrated with transmission of data from site to stakeholders via telemetry, it can allow for near-real-time monitoring of conditions as they move toward critical hydrogeological failure states.

In summary, the success of ER methods to monitoring of landslides is due to the longevity of the monitoring periods that can be achieved (e.g., Palis, Lebourg, Tric, et al., 2017), the resolution at which data sets can be acquired (e.g., Supper et al., 2014), the use of semipermanent installations of geophysical monitoring infrastructure coupled with environmental and geotechnical sensor networks (e.g., Uhlemann et al., 2017), the ability for the results to be related to subsurface properties pertinent to landslide processes (e.g., Crawford & Bryson, 2018; Lucas et al., 2017), and in some cases the ability to yield critical subsurface information with minimal postacquisition processing (e.g., Lebourg et al., 2010; Merritt et al., 2018).

5.2. Challenges to Geophysical Monitoring of Moisture-Induced Landslides

Of the methods assessed in this review, ER monitoring has the greatest potential for monitoring subsurface material properties which may lead to slope failure. This is despite limitations surrounding power supplies to instruments, the practical considerations of deploying an electrode array in topographically difficult terrain, and the limitation of high-resolution spatial information to the near surface. With regards to semipermanent ER monitoring, these issues have mostly been addressed as many of the semipermanent ER systems in this review have been developed specifically for the purpose of landslide monitoring, while other approaches have adapted existing equipment and methodologies. Further technological developments are still required in these approaches to optimize their application to landslide monitoring.

Active seismic methods (SR, SW) require the use of impulsive sources for generating seismic waves on site, limiting their use to transient measurements rather than semipermanent installations (e.g., Grandjean et al., 2009; Renalier, Jongmans, et al., 2010) as no remote impulse generators exist for this application in surface deployed arrays (Daley et al., 2007). Other methods, such as SP, seem to be less used due to potential ambiguities in data interpretation, and the heavy reliance in determining subsurface conditions, such as lithology, from other sources. However, the single example of SP monitoring by Colangelo et al. (2006) demonstrates the value of SP approaches, particularly when included as part of a wider geophysical, environmental, and geotechnical landslide monitoring campaign (Perrone et al., 2004). The passive approach provided by SP monitoring should lend itself to integration into new and existing geophysical monitoring observatories, as the infrastructure required is significantly less than that required for the establishment of ER monitoring systems.

While passive seismic methods are widely used to retrospectively analyze the patterns of seismicity associated with landslide movements, their use to monitor the evolution of subsurface conditions preceding failure is underutilized. This can be considered a missed opportunity, particularly given their ability to monitor at higher temporal resolutions than active geophysical methods, and image to greater depths (where such imaging capabilities are able to be employed, such as using S-ANT). This is despite the field of passive seismic monitoring being both highly developed and widely applied in monitoring both macroseismic (e.g., Öz, 2015)

and microseismic (e.g., Chambers et al., 2010) events in a wide range of applications, including hydraulic fracture stimulation, geothermal systems, waste storage (e.g., CO_2), and mining. Seismic monitoring is also not uncommon in landslide monitoring, most commonly for detection and analysis of rockfall failure events (e.g., Hibert et al., 2017; Manconi et al., 2016; Partsinevelos et al., 2016). Similar approaches have been undertaken in some of the case studies identified in this review, such as event classification (Palis, Lebourg, Vidal, et al., 2017) and event location (Brückl et al., 2013).

A significant challenge common to most geophysical monitoring applications remains the large volumes of data that can be acquired and the time requirements to quality assess, process, and interpret these data. Currently, most data are still assessed and processed manually, although significant strides in acquisition methods, automated filtering, and inversion methods have increased productivity in these areas (Loke et al., 2013). Challenges such as the accounting for movements in electrodes in active landslides (Wilkinson et al., 2010; Wilkinson et al., 2015) have been overcome, although similar challenges remain in the areas of automated image and pattern analysis (Chambers et al., 2015; Ward et al., 2016), the development of which would significantly reduce the requirement for manual processing of monitoring data. While robust hardware for geophysical monitoring seems to have reached good operational standards in recent years, developments in the associated software capabilities are still required to optimize the monitoring process.

5.3. Future Look and Opportunities

Currently, the only other methodology that is able to deliver robust monitoring capabilities and soil and rock property identification in a similar manner to semipermanent ER monitoring systems is long-term passive seismic monitoring campaigns. A particularly novel but promising approach to passive monitoring is the use of ambient noise monitoring at landslide sites, with studies by Harba and Pilecki (2017), Mainsant et al. (2012) and Renalier, Jongmans, et al. (2010) demonstrating particularly interesting results. The predictive capacity of using cross correlations of ambient noise is made clear in the study by Mainsant et al. (2012), where relative velocities in surface waves are seen decreasing days before slope failure. Critically, this failure did not seem to be linked to obvious changes in the rainfall regime, suggesting that a long-term retrospective establishment of threshold values from rainfall data would not have worked in this landslide setting. The production of subsurface images of *S* wave velocity from ambient noise recordings by Harba and Pilecki (2017) also shows that passive monitoring methods can determine subsurface properties and produce images at similar spatial resolutions to transient SR and SW surveys. However, improvements to the methodology described in Harba and Pilecki (2017) could improve the robustness of the results. Ambient noise sources ideally need to be both stable in time and nondirectional, although the former can be overcome by averaging over increased measurement times (e.g., Mainsant et al., 2012). In the case study by Harba and Pilecki (2017), the acquisition of 60-min data sets derived from traffic noise may not be sufficient to reliably reconstruct the Green's function of an ambient noise field. Accurate reconstruction of the Green's function is crucial due to the accuracy of the imaging capability. The deployment of permanent arrays, from which longer ambient noise records could be extracted, would greatly improve the reliability of the results. Despite this, the case study by Harba and Pilecki (2017) is one of the only attempts to create subsurface images from ambient noise for the purpose of monitoring landslides. As such, it represents an important step in providing increased temporal and spatial subsurface geophysical models of landslides, and demonstrates the capacity for employing such approaches in future studies.

Crucially, unlike transient SR and SW surveys, subsurface images produced from ambient noise have the potential to be produced at a similar acquisition frequency to long-term semipermanent ER monitoring systems. Recent developments in technology, particularly around linear Distributed Acoustic Sensing monitoring, show the potential for these new senor types to replicate the resolution of traditional transient SW surveys, but at much higher data acquisition frequencies (Dou et al., 2017). Developments in this field, potentially into 3-D surveys, will be particularly relevant to the monitoring of landslides. Renalier, Bievre, et al. (2010) demonstrate the application of these ambient noise applications using a network of seismometers to create a 3-D image of a landslide body, but without a time series element to the data. Similarly, while some nonmonitoring studies have analyzed seismic data and inferred property distributions from active seismic measurements (Uhlemann, Hagedorn, et al., 2016), this has not been applied to time-lapse seismic studies, actively or passively acquired, and represents a significant gap in the field.

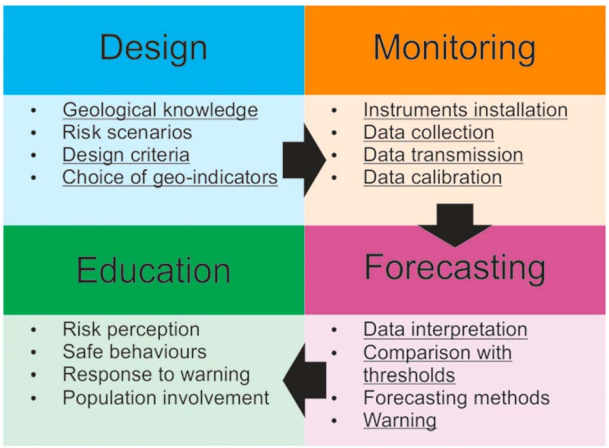

Figure 13. Four main activities of landslide early warning systems (EWS) reproduced from Intrieri et al. (2013). Sections underlined show the areas in which geophysical investigations and/or geophysical monitoring can be used to assist in landslide EWS.

Therefore, there appears to be three areas in which seismic monitoring can be improved for the application of monitoring landslides: by utilizing ambient data sets acquired by dense seismometer networks or Distributed Acoustic Sensing arrays over longer periods of time, by attempting to link changes observed in these data sets to subsurface properties, and by producing high-resolution spatial images of the subsurface from passive data. In the past, a barrier to improving resolution of ambient noise surveys has been the cost associated with broadband seismometers typically used for very sensitive planetary-scale measurements. However, recent studies in other areas show the successful deployment of low-cost, low-energy consumption geophone-based networks for the monitoring of glaciers (Martinez et al., 2017), infrastructure (Olivier et al., 2017; Salvermoser et al., 2015), and landslides (Deekshit et al., 2016). Similar moves toward lower-power, lower-cost systems in ER monitoring are also apparent (Chambers et al., 2016), which will increase the availability and application of geophysical monitoring in the field.

The simultaneous acquisition of continuous passive seismic and ER data would open up opportunities for the further development of integrated quantitative processing and inversion, further increasing the usefulness of geophysical monitoring data. The near-real-time element of some monitoring systems could therefore be used for near-time modeling and decision making on high-risk slopes endangering critical social or economic infrastructure, or risk to human life.

5.4. The Contribution of Geophysical Methods to Landslide EWS

The compilation of catalogs of landslide events is often the first step to constructing landslide inventory maps. These maps inform the designation of zones based on their level of risk to landslide events (Fell et al., 2008; van Westen et al., 2006). Implementation of appropriate land use planning and subsequent enforcement of this planning is arguably the most effective tool for mitigating future risk from landslide events, and can be practiced at different scales (Cascini, 2008). However, in some situations, the presence of risk from landslides may exist in the absence of appropriate risk zonation maps, or may become apparent in the later development of land. Changing environmental conditions can also induce new landslide events, or reactivate dormant landslide activity (Gariano & Guzzetti, 2016). In these instances, different courses of action must be taken to mitigate the risk from future landslide events.

In cases where the elements at risk of a landslide hazard cannot be relocated, or are of high socioeconomic value (Manconi & Giordan, 2015) or where structural mitigation measures would be too resource intensive, undesirable, or ineffective, the implementation of early warning systems (EWS) may be the preferred option for risk mitigation (Intrieri et al., 2012). EWS applied to natural hazards can be defined as "… monitoring devices designed to avoid or to mitigate the impact posed by a threat" (Medina-Cetina & Nadim, 2008). Slope-scale EWS for landslide monitoring requires a detailed understanding of the triggers and mechanisms in order to be effective (e.g., Manconi & Giordan, 2016). Successful slope-scale EWS must include a detailed understanding of the character of the landslide, the processes acting on the slope, and the response of the slope to external influences, such as increased infiltration (SafeLand, 2012). The main components of EWS are shown in Figure 13.

Typically, slope-scale EWS are established by acquiring and monitoring changes in both environmental (i.e., rainfall, temperature, soil moisture content, pore water pressure) and kinematic (i.e., slope movement) data (Uhlemann, Smith, et al., 2016). Commonly, these data that are acquired through geomorphological mapping, geodetic surveys, and borehole measurements (e.g., inclinometers) are used in monitoring campaigns. Data can also be acquired from sensors measuring piezometric head, tilt, and soil suction. More recently, wireless sensor networks comprising sensors with low-power requirements and large data storage or telemetric capabilities have been deployed in landslide settings to acquire direct measurement data with higher spatial and temporal resolution (Ramesh, 2014). Despite these advances, logistical and economic constraints remain barriers to optimum data acquisition for the establishment of effective EWS. Currently, geophysical investigations and monitoring methods are not widely used in slope-scale landslide EWS.

Table 3
The Contributions That Geophysical Monitoring Approaches Can Make to EWS in the Context Proposed by Intrieri et al. (2013) in Figure 13

EWS Activity (After Intrieri et al., 2013)		Contribution by Geoelectrical Monitoring Methods	Contribution by Passive Seismic Monitoring Methods
Monitoring	Instruments installation	Installation of semipermanent 2-D monitoring arrays	Installation of seismometer(s)
		Installation of semipermanent 3-D monitoring arrays	Installation of dense networks of low-cost, low-power seismic sensors or DAS arrays
	Data collection	Regular, short-time scale (≤1 day) data acquisition	Continual data recording
		Large data storage or telemetric capabilities	
	Data transmission	Telemetric capability can send data to central observatory	
	Data elaboration	Integration of data with environmental, geotechnical and kinematic data collected simultaneously from locally installed sensors	
Forecasting	Data interpretation	Automatic image analysis and change detection of hydrogeological process through time-lapse imaging	Automatic seismic event detection
		Automated geotechnical coupled and environmentally coupled monitoring	Automated event classification
			Automated event location
	Comparison with thresholds	Establishment of relevant subsurface hydrogeological thresholds preceding movement (e.g., moisture content, shear strength)	
	Forecast methods	Monitoring of subsurface conditions toward hydrogeological failure threshold	Monitoring of subsurface conditions toward geomechanical failure threshold
	Warning	High-resolution spatial and temporal geophysical monitoring, calibrated with and linked to environmental, geotechnical, and kinematic data to provide multilevel warnings based on monitoring of several physical subsurface parameters	

Note. Those contributions highlighted red indicate areas in which the most development is still required, those in orange are where research is currently being undertaken but not yet applied to the monitoring of MIL, and green identifies those areas in which geophysical monitoring can already contribute the slope-scale EWS on MIL.

Table 3 shows the contribution that geophysical monitoring approaches can make to the four stages of establishing landslide EWS, as defined by Intrieri et al. (2013) and shown in Figure 13. Entries highlighted green are those areas in which capability has been demonstrably developed. Orange entries indicate those areas in which challenges still exist but where the requisite technology may have been applied to other areas of geophysical monitoring outside of landslide studies, for example, in the automatic detection of geophysical responses, and installation of high-resolution monitoring arrays. Entries in red indicate areas in which significant development is still required before operational deployment to a field setting, the most significant one of which being the ability to issue reliable warnings based on the integration of environmental, geotechnical, and geophysical data.

6. Conclusions

The use of geophysical monitoring systems to assess the evolution of subsurface property distributions and changes over time have been reviewed. The benefit of long-term geophysical monitoring campaigns in assessing the evolution of MIL is demonstrable. A significant advantage of the use of geophysical monitoring systems is their complementarity with existing monitoring systems. Many areas of landslide monitoring are highly developed, with innovative advances in technology progressing a wide range of applications. Developments in UAV technology (Walter et al., 2009), interferometric synthetic-aperture radar (Hilley et al., 2004), and other remote sensing capabilities (Kirschbaum et al., 2015) have increased the temporal and spatial resolution at which surface deformations can be monitored. Geophysical data can enhance the deformation data captured by these technologies by providing an understanding of the subsurface processes driving them, something that is not achievable at such high temporal and spatial resolutions with other monitoring methods. Sensor technology has also advanced, with installations of tiltmeters, inclinometers, and piezometers being enhanced with the addition of shape acceleration arrays, acoustic-emission waveguide sensors, and tensiometers (Uhlemann, Smith, et al., 2016). Geophysical methods are able to interpolate between the locations of these direct measurements, extending by proxy the spatial coverage of these sensor types.

Key advances in the field of geophysical monitoring in the last decade include the following:

Table A1
Published Case Studies Utilizing Geophysical Monitoring of Landslides Since 2006 With Information on the Landslide Setting

Authors	Landslide name and location	Approximate depth to slide (m bgl)	Approximate slope angle (°)	Approximate area (m^2)	Movement type (after Hungr et al., 2014)	Material
Brückl and Mertl (2006)	Gradenbach Schober Range, Carinthia, Eastern Alps, Austria			$1.68x10^6$	Mountain slope deformation	Phyllites and calcareous mica schists
Brückl and Mertl (2006)	Hochmais-Atemskopf Ötztaler Alpen, Tyrol, Eastern Alps, Austria			$2.82x10^6$	Mountain slope deformation	Paragneisses, micaschists, orthogneisses, amphibolites
Brückl and Mertl (2006)	Niedergallmigg-Matekopf Samnaun Range, Tyrol, Eastern Alps, Austria			$2.64x10^6$	Mountain slope deformation	Pelitic genisses, micaschists
Colangelo et al. (2006)	Varco d'Izzo Potenza, Basilicata, Southern Apennine, Italy	15 – 25	8 – 16	$1.82x10^5$ – $5.88x10^5$	Composite rotational-translational -flow	Clay-marl terrains, including blocks of marls, calcarenites and limestones
Friedel et al. (2006)	Toessegg Banks of Rhine, Rüdlingen, Switzerland	0.6 – 1.5	20 – 30	-	Translational	Quaternary deposits overlying sandstone
Amitrano et al. (2007)	Super-Sauze Barcelonette Basin, Southeast Alps, France	5 – 10	25	-	Slide - flow	Weathered marl (clay)
Jomard et al. (2007)	La Clapière Alpes Maritimes, France	10	40	-	Translational - rotational	Fractured gneiss
Bell et al. (2008)	Lichenstein-Unterhausen Swabian Alps,south Germany	ILEWS Project update.				
Walter and Joswig (2008)	Heumoes Vorralberg Alps, Austria		-	$9x10^5$	Slide	Loamy scree and till (silty, clayey and sandy material)
Grandjean et al. (2009)	Laval Laval catchment, ORE, Draix, South French Alps	5	30	$4x10^3$	Slide-flow?	Weathered marls
Walter et al. (2009)	Super-Sauze Barcelonette Basin, Southeast Alps, France	Described in more detail by Walter et al. (2012)				
Helmstetter and Garambois (2010)	Séchilienne Belledonne massif, French Alps, France	-	35 - 40	-	Rockslide	Mica schists with interbedded quartz-feldspar layers
Lebourg et al. (2010)	Vence Alps Maritimes, South East France	12	12 – 14	$8.75x10^4$	Translational	Sandy-clay overlying marls
Renalier et al. (2010a)	Avignonet Trièves area, French Alps, France	5 – 42	8 – 15	$1.5x10^6$	Translational rotational -	Lacustrine and alluvial clay
Gomberg et al. (2011)	Slumgullion San Juan mountains, Colorado, United States	20	-	$1.17x10^6$	Translational	Sandy, silty clay and areas of bouldery debris, clay and pond and stream sediment
Lacroix and Helmstetter (2011)	Séchilienne Belledonne massif, French Alps, France	-	35 - 40	-	Rockslide	Mica schists with interbedded quartz-feldspar layers
Walter et al. (2011)	Heumoes Vorralberg Alps, Austria	-	-	$9x10^5$	Slide	Loamy scree and till (silty, clayey and sandy material)
Bièvre et al. (2012)	Avignonet Trièves area, French Alps, France	5 – 42	8 – 15	$1.5x10^6$	Translational rotational -	Lacustrine and alluvial clay
Luongo et al. (2012)	- Picerino region, Basilicata region, Italy	-	-	-	Translational rotational -	Schist, flysch

Table A1 *(continued)*

Authors	Landslide name and location	Approximate depth to slide (m bgl)	Approximate slope angle (°)	Approximate area (m^2)	Movement type (after Hungr et al., 2014)	Material
Mainsant et al. (2012)	Pont Bourquin Switzerland	"few metres" to 11	-	$8x10^3$ *(potentially $3x10^4$ – $4x10^4$*	Active composite earthslide - earthflow	Triassic dolomites and gypsum, with flysch deposits mid-slope, including siltstones and conglomerates
Travelletti et al. (2012)	Laval Laval catchment, ORE, Draix, South French Alps	1 – 6	32	$4x10^3$	Slide-flow?	Weathered marls
Walter et al. (2012)	Super-Sauze Barcelonette Basin, Southeast Alps, France	5 – 10	25	-	Slide - flow	Weathered marl (clay)
Brückl et al. (2013)	Gradenbach Schober Range, Carinthia, Eastern Alps, Austria	-	-	$1.7x10^6$		Phyllite, schists and carbonates
Lehmann et al. (2013)	Controlled site Banks of Rhine, Rüdlingen, Switzerland	0.7 – 5.6	38	262.5	Slide?	Silty sandy clay overlying marlstones and sandstones
Tonnellier et al. (2013)	Super-Sauze Barcelonette Basin, Southeast Alps, France	5 – 10	25	-	Slide - flow	Weathered marl (clay)
Tonnellier et al. (2013)	Valoria Northern Appenines, Dolo River Basin, Italy	15 – 30?	-	$1.6x10^6$	Translational slide?	Flysch and clay-shale
Walter et al. (2013)	Heumoes Vorralberg Alps, Austria		-	$9x10^5$	Slide	Loamy scree and till (silty, clayey and sandy material)
Walter et al. (2013)	Slumgullion San Juan mountains, Colorado, United States	Study described in Gomberg et al. (2011)				
Walter et al. (2013)	Super-Sauze Barcelonette Basin, Southeast Alps, France	Study described in Walter et al. (2009)				
Supper et al. (2014)	Ampflwang-Hausruck Ampflwang, Hausruck Hills, Austria	20 – 30	-	$4.4x10^3$	Rotational-translational	Quaternary colluvium, anthropogenic deposits and Neogene
Supper et al. (2014)	Bagnaschino Torre Mondovì, Casotto Valley, Cuneo/ Piedmont Province, Italy	8	-	1.5×10^5	Rotational-translational	Colluvium overlying amphibolite and schist
Kremers et al. (2015)	Badong China	YANGTZE-GEO project update.				
Jongmans et al. (2015)	Pont Bourquin Switzerland	Summary of Mainsant et al., 2012.				
Gance et al. (2016)	Super-Sauze Barcelonette Basin, Southeast Alps, France	~5? "a few metres"	25	-	Slide - flow	Weathered marl (clay)
Harba and Pilecki (2017)	Just-Tegoborze Nowy Sacz, Southern Poland	10 – 12 and 14 - 17	-	-	-	Colluvial deposits overlying flysch deposits
Xu et al. (2016)	Bank of Zagunao River Lixian County, Sichuan Province, China	30 – 70	25 -35	$1.06x10^6$	-	Colluvial deposits overlying Devonian phyllite
Imposa et al. (2017)	Tripi, north-eastern Siciliy, Italy	4-Mar	-	$2.49x10^3$	Translational?	Colluvial deposits overlying paragneiss
Lucas et al. (2017)	Canton of Valais, Swiss Alps, Switzerland	3-Jan	33 - 43	-	-	Gravels, silt and sand overlying quartzite bedrock
Palis et al. (2017a)	La Clapière Alpes Maritimes, France	<100-200? (Jomard et al., 2010)	-	$>8x10^5$	Rockslide	Granodiorite and migmatitic gneiss
Palis et al. (2017b)	Vence	15-Oct	14-Dec	$8.75x10^4$	Translational (Lebourg et al., 2010)	Sandy clay overlying Jurassic limestone

Table A1 *(continued)*

Authors	Landslide name and location	Approximate depth to slide (m bgl)	Approximate slope angle (°)	Approximate area (m^2)	Movement type (after Hungr et al., 2014)	Material
Provost et al. (2017)	Alps Maritimes, South East France Super-Sauze Barcelonette Basin, Southeast Alps, France	~5? "a few metres"	25	-	Slide - flow	Weathered marl (clay)
Uhlemann et al. (2017)	Hollin Hill North Yorkshire, UK	3-Feb	12	$3.9x10^4$	Composite earth-slide earth-flow	Weathered mudstones and sandstones
Crawford and Bryson, 2018	Doe Run Kentucky, USA	<8	-	$2.5x10^3$	Translational	Silty clay colluvium overlying shale and limestone
Crawford and Bryson, 2018	Herron Hill Kentucky, USA	<3	-	$3.75x10^4$	Composite rotational translational?	Silty Clay colluvium and weathered shale
Merritt et al., 2018	Hollin Hill North Yorkshire, UK	3-Feb	12	$3.9x10^4$	Composite earth-slide earth-flow	Weathered mudstones and sandstones

Note. ER electrical resistivity; SW surface wave methods; SP self-potential; SR seismic refraction; S-EDCL continuous seismic monitoring, including use of event characterization, detection, and location methods; S-H/V seismic monitoring utilizing horizontal-to-vertical ratio methods; S-CC seismic monitoring utilizing cross-correlation methods; S-ANT seismic monitoring utilizing ambient noise tomography methods.

1. Telemetric capabilities in geoelectrical and seismic monitoring methods, increasing the length of monitoring periods and allowing near-real-time data acquisition.
2. Coupling of geophysical data to geotechnical properties, particularly in the field of ER.
3. The potential for integration of passive seismic and ER methods to decrease uncertainty in single-method geophysical monitoring campaigns.

A key area for future development is the implementation of multiparametric monitoring with geotechnically coupled approaches. This can be achieved through better calibration of geophysical measurements with geotechnical data, and the establishment of threshold values for failure based on these outputs.

Recent advances in incorporating slope displacements in the data processing phase of geophysical monitoring campaigns has greatly reduced the presence of artifacts in the resultant subsurface images (Wilkinson et al., 2010; Wilkinson et al., 2015), as well as advances in the inversion of time-lapse data (Loke et al., 2013) and automated image analysis (Chambers et al., 2015; Ward et al., 2016). The establishment of site-specific geotechnical-geophysical relationships to obtain the subsurface spatial distribution of geotechnical properties, and the ability to monitor changes in these properties over time, is valuable to a wide range of end-users and stakeholders (Crawford & Bryson, 2018; Merritt et al., 2016; Uhlemann et al., 2017). The developments highlighted in this review underscore the potential for the combined use of geophysical monitoring methods with existing remote sensing, Earth observation, and direct measurement monitoring approaches to improve the current capacity for high-resolution slope-scale landslide EWS (Intrieri et al., 2012; Intrieri et al., 2013).

Appendix A

This table lists all the case studies identified as part of this review. Studies were selected for their use of geophysical monitoring approaches to study landslides as (see text). Where possible, further information regarding the landslide setting has been extracted from the case study text. A brief summary of the key findings of the study is found in the "notes" column (Table A1).

Glossary

Cascading Disaster: As defined by Pescaroli and Alexander (2015), these are "… extreme events, in which cascading effects increase in progression over time and generate unexpected secondary events of strong

Table A2
Published Case Studies Utilizing Geophysical Monitoring of Landslides Since 2006 With Information on Geophysical Monitoring

Authors	Geophysical monitoring method	Monitoring type	Dimension	Monitoring period (Days)	Number of datasets/ seismometers*	Survey design	Notes
Brückl and Mertl (2006)	S-EDCL	Semi-permanent		15	8*		Detected, characterised and located seismic events on the slope-scale at a slowly deforming rock mass.
	S-EDCL	Semi-permanent		1	9*		
	S-EDCL	Semi-permanent		10	8*		
Brückl and Mertl (2006)	S-EDCL	Semi-permanent		?	5*		
	S-EDCL	Semi-permanent		19	2*		
	S-EDCL	Semi-permanent		5	11*		
Brückl and Mertl (2006)	S-EDCL	Semi-permanent		9	5*		
Colangelo et al. (2006)	SP	Controlled test	2D	1	8	1 x 50m profile (11 electrodes at 5m spacing	Only SP monitoring case study. Showed time-lapse SP tomograpic images indicating subsurface flow. The 24 hour monitoring period was part of a longer semi-permanent monitoring campaign.
Friedel et al. (2006)	ER	Transient	2D	336	2	1 x 24.5m profile (50 electrodes at 0.5m spcaing	Comparative analysis of ER tomographic images acquired one year apart showed influence of rainfall.
Amitrano et al. (2007)	S-H/V	Semi-permanent	1D	13	1*	1 seismometer	H/V ratio from a single seismometer shown in response to landslide movement.
Jomard et al. (2007)	ER	Controlled test	2D	2	14	1 x 141m profile (48 electrodes at 3m spacing	Time-lapse ER tomographic images showed moisture changes over period of controlled rainfall experiment.
Bell et al. (2008)	ILEWS Project update.						
Walter and Joswig (2008)	S-EDCL	Semi-permanent	1D	7	8	Two tripartite sensor arrays deployed in each period, comprising of 1 x 3-component sensor surrounded by 3 x 1-component sensors	Two monitoring periods in rapid succession (nine days separation) showed increase in nanoseismic activity five to 26 hours after rainfall event.
	S-EDCL	Semi-permanent		7	8		
Grandjean et al. (2009)	ER	Controlled test	2D	2.8	32	1 x 47m profile (48 electrodes at 1m spacing	Controlled rainfall experiment, presented statistical time-laspe images produced from ER and SR data. Same experiment as in (Travelletti et al., 2012).
	SR	Controlled test	2D	2.8	23	1 x 47m profile (48 geophones at 1m spacing	
Walter et al. (2009)	Described in more detail by Walter et al. (2012)						
Helmstetter and Garambois (2010)	S-EDCL	Semi-permanent	1D	715	45	3 x sensor arrays comprising of 6 vertical and 1 3 component arrays	Two years of seismic event detection, classification and detection showed a weak, but

Table A2 *(continued)*

Authors	Geophysical monitoring method	Monitoring type	Dimension	Monitoring period (Days)	Number of datasets/ seismometers*	Survey design	Notes
						(all replaced by broadband sensors in 2009) and an additional 24 channel geophone array installed in 2008.	significant, correlation of rockfall events with rainfall, with even 1mm of rain showing an increase in seismically-detected rockfall events, although events still occurred in the absence of rainfall.
Lebourg et al. (2010)	ER	Semi-permanent	2D	90	90	1 x 115m profile (24 electrodes at 5m spacing	Used statistical analysis of resistivity data to correlate with rainfall.
Renalier et al. (2010a)	S-CC	Semi-permanent	2D	944	2*	2 seismometers from larger array	Cross-correlation between seismometer pair demonstrated landslide movement by using seismic arrival times.
Gomberg et al. (2011)	S-EDCL	Semi-permanent	2D	9	88*		Some issues with instrument batteries in achieving full monitoring coverage with complete network, but at least 2 days complete monitoring achieved. Determined movement occurs both seismically and aseismocally at the Slumgullion landslide.
Lacroix and Helmstetter (2011)	S-EDCL	Semi-permanent	2D	425	45	3 x sensor arrays comprising of 6 vertical and 1 3 component arrays (all replaced by broadband sensors in 2009) and an additional 24 channel geophone array installed in 2008.	Focuses on locating seismic events within the Séchilienne rockslide associated with rockfalls and basal movements, the latter causing microearthquakes. Some areas showed aseismic movements.
Walter et al. (2011)	S-EDCL	Semi-permanent		<28	8*	Two tripartite sensor arrays deployed, comprising of 1 x 3-component sensor surrounded by 3 x 1-component sensors	Extension of Walter and Joswig (2008). Monitoring periods of one to four weeks were undertaken in 2005, 2006, 2007 and 2008. Showed continued increase of seimsic activity five to 26 hours after rainfall events, presumed to be linked to moisture-induced failure.
	S-EDCL	Semi-permanent		<28	8*	Two tripartite sensor arrays deployed, comprising of 1 x 3-component sensor surrounded by 3 x 1-component sensors	
	S-EDCL	Semi-permanent		<28	12*	Three tripartite sensor arrays deployed, comprising of 1 x 3-component sensor surrounded by 3 x 1-component sensors	
	S-EDCL	Semi-permanent		<28	20*	Five tripartite sensor arrays deployed, comprising of 1 x 3-component sensor surrounded by 3 x 1-component sensors	
Bièvre et al. (2012)	ER	Transient	2D	498	4	1 x 31.5m profile (64 electrodes at 0.5m spacing	Focused on hydrological infiltration through fissures.

Table A2 *(continued)*

Authors	Geophysical monitoring method	Monitoring type	Dimension	Monitoring period (Days)	Number of datasets/ seismometers*	Survey design	Notes
							Fissures identified through time-lapse ER tomographic images, and size of fissures over time assessed using SW methods.
	SW	Transient	1D	198	2	1 x 57.5m profile (24 geophones at 2.5m spacing	
Luongo et al. (2012)	ER	Semi-permanent	2D	146	584	1 x 47m profile (48 electrodes at 1m spacing	Preliminary study of time-lapse ER monitoring instrument on shallow landslide.
Mainsant et al. (2012)	S-CC	Semi-permanent	2D	146	2*	2 seismometers	Used cross-correlation of ambient noise records to detect relative decreases in landslide material strength before failure.
Travelletti et al. (2012)	ER	Controlled test	2D	2.8	32	1 x 47m profile (48 electrodes at 1m spacing	Identified steady-state flow conditions in a controlled rainfall experiment using time-lapse ER tomographic images, and estimated steady-state flow from ER.
Walter et al. (2012)	S-EDCL	Semi-permanent		10	16*	Four tripartite sensor arrays deployed, comprising of 1 x 3-component sensor surrounded by 3 x 1-component sensors	Discriminated between seismic events associated with rock falls, and slide movement ('slidequakes'). Slidequakes were able to be located within the moving body of the landslide, and the highest amplitude events associated with period after rainfall. Signifcant attenuation linked to surface fissure development.
Brückl et al. (2013)	S	Semi-permanent	1D	212	6*	6 seismometers	Used seismometers to detect seismic events associated with movement, and located events, including events preceding slope failure.
Lehmann et al. (2013)	ER	Controlled test	2D	0.625	18	1 x 47m profile (48 electrodes at 1m spacing	Two controlled rainfall experiments. Compared soil wetting as measured by sesnsors and ER measurements, and showed wetting front evolution through time-lapse images.
	ER	Controlled test	2D	3	77	1 x 47m profile (48 electrodes at 1m spacing	
Tonnellier et al. (2013)	S-EDCL	Semi-permanent		14	7*	One tripartite sensor array deployed, comprising of 1 x 3-component sensor surrounded by 6 x 1-component sensors	First period (14 days) targetted small displacements, second (28 days) targetted moderate displacements. Compared to measurements at Valoria (see below). Located quakes associated with moving inshearing zone. Potential slow-slip seismic noise was identified. Low-correlation between increased seismic activity and landslide acceleration, but good correlation between increased seismic activity and heavier rainfall.
Tonnellier et al. (2013)	S-EDCL	Semi-permanent		10	14*	Two tripartite sensor arrays deployed, comprising of 1 x 3-component sensor	Targetted large displacements, and compared to measurements from Super-Sauze (see above). Identified events associated with

Table A2 *(continued)*

Authors	Geophysical monitoring method	Monitoring type	Dimension	Monitoring period (Days)	Number of datasets/ seismometers*	Survey design	Notes
						surrounded by 6 x 1-component sensors	material deformation. Potential slow-slip seismic noise was identified. Correlated increased seismic activity with increased acceleration of slide.
Walter et al. (2013)	S-EDCL	Semi-permanent		700	12*	Three tripartite sensor arrays deployed, comprising of 1 x 3-component sensor surrounded by 6 x 1-component sensors	Comparison of slidequake generation at three different landslide settings. Two of the sites (Super-Sauze and Slumgullion) reproduced data from previous studies, but data from Heumoes is from long-term permanent array installation installed July 2008, following on from intermittent studies detailed in Walter et al. (2011). Study was able to determine conditions leading to brittle failure in several landslide settings.
Walter et al. (2013)	Study described in Gomberg et al. (2011)						
Walter et al. (2013)	Study described in Walter et al. (2009)						
Supper et al. (2014)	ER	Semi-permanent	2D	275	1650	1 x 60m profile (61 electrodes at 1m spacing	Showed time-lapse ER tomomgaphic images over periods of varying seasonal rainfall and snow melt.
Supper et al. (2014)	ER	Semi-permanent	2D	239	1434	1 x 224m profiles; varying electrode spacing (1m spacing in centre, increasing at edges	Showed time-lapse ER tomographic images of a movement event.
Kremers et al. (2015)	YANGTZE-GEO project update. Summary of Mainsant et al., 2012.						
Jongmans et al. (2015)							
Gance et al. (2016)	ER	Semi-permanent	2D	284	568	1 x 113m profile (93 electrodes with varying spacings of 0.5m, 1m and 2m	Used time-lapse ER tomographic images to analyse response of subsurface to two natural rainfall events, highlighting importance of thermal exchange in ER monitoring.
Harba and Pilecki (2017)	S-ANT	Transient	2D	167	12*	12 seismometers along two profiles 1 x 75m and 1 x 95m	Inverted ambient noise records to produce tomographic images of shear wave velocity. Comparative image analysis showed changes in slip surface and moisture content.
Xu et al. (2016)	ER	Transient	2D	274	6	3 x 595m profiles (120 electrodes at 5m spacing	Presented time-lapse ER tomographic images to create a hydrogeological model of landslide mass.
Imposa et al. (2017)	S-H/V	Transient	2D	1589	68	34 H/V stations across profiles	Compared H/V profile from a landslide 5 years apart to detect changes in sliding surface.
Lucas et al. (2017)	ER	Transient	2D	62	6	1 x 47m profile (48 electrodes at 1m spacing	Used time-lapse ER tomographic images to compare areas of increasing and decreasing

Table A2 *(continued)*

Authors	Geophysical monitoring method	Monitoring type	Dimension	Monitoring period (Days)	Number of datasets/ seismometers*	Survey design	Notes
							saturation. Compared volumetric water content measured by ER and sensors, and showed slight over estimation from ER measurements.
Palis et al. (2017a)	ER	Semi-permanent	2D	365	365	1 x 235m profile (48 electrodes at 5m spacing	Seismic monitoring focused on event classification. Apparent ER data clustered identified sliding mass.
	S	Semi-permanent	1D	365	1*	1 seismometer	
Palis et al. (2017b)	ER	Semi-permanent	2D	3510	3510	1 x 115m profile (24 electrodes at 5m spacing	Clustered apparent ER data to look at long-term trends of different units in response to rainfall over 9.5 year period.
Provost et al. (2017)	S-EDCL	Semi-permanent		40	8*	Two tripartite sensor arrays deployed, comprising of 1 x 3-component sensor surrounded by 6 x 1-component sensors	Tested automatic classification methods for detection of events associated with movement.
	S-EDCL	Semi-permanent		21	8*		
	S-EDCL	Semi-permanent		68	8*		
Uhlemann et al. (2017)	ER	Semi-permanent	3D	1369	658	5 x 147.25m profiles (32 electrodes at 4.75m spacing and 9.75m between profiles	Presented time-lapse 3D ER tomographic images, and derived gravimetric moisture content from ER data, showing seasonal gravimetric moisture content changes.
Crawford and Bryson, 2018	ER	Transient	2D	350	5	2 x ~56.7m profiles (64 electrodes at 0.91m spacing)	Presented relative changes in resistivity linked to rainfall, and resistivity results linked to shear strength parameters; shear strength plotted to produce shear strength profile.
Crawford and Bryson, 2018	ER	Transient	2D	350	5	3 x ~62.8m profiles (69 electrodes at 0.91m spacing)	Presented relative changes in resistivity linked to rainfall, and resistivity results linked to shear strength parameters.
Merritt et al., 2018	ER	Semi-permanent	1D	1740	695	4 x time-lapse contact resistance points	Contact resistances used, extracted from larger ER monitoring array (Uhlemann et al., 2017).

impact. These tend to be at least as serious as the original event, and to contribute significantly to the overall duration of the disaster's effects."

Cohesion: In Mohr-Coulomb failure, cohesion is the component of the shear strength of a material that is not caused by interparticle friction, and instead arises from electrostatic forces and cementing. Apparent cohesion can also be caused by the presence of negative pore water pressures, or soil suction.

Element at Risk: Any person, property, infrastructure, or other socioeconomic unit that is exposed to a hazard.

Green's Function: Green's functions describe the energy between pairs of seismic receivers, if one of the receivers was an impulsive source. They therefore relate to the condition of the medium a seismic wave has traveled through.

Landslide Inventory Map: A map detailing the location, extents, and types of landslides, used for the purposes of hazard zoning. Landslide inventory maps may be created using a "top-down" approach, that is,

identifying all landslides within a set area, or a "bottom-up" approach, that is, identifying the hazard posed by a single landslide and identifying other similar hazards in an area.

Phase Velocity: The velocity at which waves within a particular frequency envelope travel in a media, with the principle being that different frequency waves generated from the same source may move at different velocities.

Piezometer: An instrument for measuring pore water pressure and identifying piezometric head. The piezometric head represents a surface of equal water pressure, which in an unconfined system would coincide with the top of the water table.

Pore Water Pressure: The pressure of water residing in the interparticle pore spaces of a soil or rock. Pore water pressures can be negative (known as "soil suction"), in which state they tend to increase the restraining forces against slope failure, by increasing cohesion and therefore the shear strength of a soil. Positive pore water pressures contribute to destabilizing forces in slope failure, by decreasing the effective strength of a soil.

Rainfall Threshold: A value, usually in terms of amount of precipitation over time, at which failure of a landslide is likely to occur. Increased volumes, extended periods, or a combination of these may contribute to the determination of a rainfall threshold.

Rayleigh Wave: A type of seismic surface wave that excites a retrograde elliptical motion in the ground. Analysis of Rayleigh waves typically involves creating dispersion curves of phase velocity, instead of the first-arrival times used in seismic refraction surveys.

Slidequake: A term by Gomberg et al. (1995) that describes seismic events generated by the motion of landslides, rather than from sources outside of the landslide system (e.g., earthquakes, rockfalls, ambient noise).

Soil Moisture Content: A measure of the water content of a mass of soil, usually expressed in terms of volumetric moisture content (VMC) or gravimetric moisture content (GMC). Soil moisture content is determined by measuring the volume (for VMC) or weight (for GMC) of a soil sample, before drying and reacquiring the weight or volume to determine the change in the respective measurement.

Soil Suction: The contribution to cohesive (and therefore restraining) forces generated by negative pore water pressures in a soil.

Tensiometer: A type of sensor used to measure pore water pressures, including negative pore water pressure or soil suction.

Tiltmeter: A type of sensor used to measure very subtle inclinations from the vertical that indicate deformation.

Acknowledgments
The authors would like to thank Fabio Florindo (Editor in Chief, Reviews of Geophysics) and six anonymous reviewers for their insightful comments and helpful suggestions. This work was funded by a NERC GW4+ UK Doctoral Training Partnership Studentship (grant NE/L002434/1) and in part by the BGS University Funding Initiative (S337), which are gratefully acknowledged. Jonathan Chambers and Paul Wilkinson publish with the permission of the Executive Director, British Geological Survey (UKRI-NERC). No new data were produced in the formation of this review, and all data used are cited in the reference list.

References

Acerra, C., Alguacil, G., Atakan, K., Azzara, R., Bard, P.-Y., Blarel, F., et al. (2002). Site effects assessment using ambient excitations.

Al-Saigh, N. H., & Al-Dabbagh, T. H. (2010). Identification of landslide slip-surface and its shear strength: A new application for shallow seismic refraction method. *Journal of the Geological Society of India*, *76*(2), 175–180. https://doi.org/10.1007/s12594-010-0092-y

Amitrano, D., Gaffet, S., Malet, J.-P., & Maquaire, O. (2007). Understanding mudslides through micro-seismic monitoring: The super-Sauze (south-east French Alps) case study. *Bulletin de la Societe Geologique de France*, *178*(2), 149–157. https://doi.org/10.2113/gssgfbull.178.2.149

Angeli, M.-G., Pasuto, A., & Silvano, S. (2000). A critical review of landslide monitoring experiences. *Engineering Geology*, *55*(3), 133–147. https://doi.org/10.1016/S0013-7952(99)00122-2

Arnone, E., Noto, L. V., Lepore, C., & Bras, R. L. (2011). Physically-based and distributed approach to analyze rainfall-triggered landslides at watershed scale. *Geomorphology*, *133*(3-4), 121–131. https://doi.org/10.1016/j.geomorph.2011.03.019

Baroň, I., & Supper, R. (2013). Application and reliability of techniques for landslide site investigation, monitoring and early warning—Outcomes from a questionnaire study. *Natural Hazards and Earth System Sciences*, *13*(12), 3157–3168. https://doi.org/10.5194/nhess-13-3157-2013

Barton, N. (2007). *Rock Quality, Seismic Velocity, Attenuation and Anisotropy*. London UK: CRC Press.

Bell, A. F. (2018). Predictability of landslide timing from quasi-periodic precursory earthquakes. *Geophysical Research Letters*, *45*, 1860–1869. https://doi.org/10.1002/2017GL076730

Bell, R., Thiebes, B., Glade, T., Vinogradov, R., Kuhlmann, H., Schauerte, W., et al. (2008). The technical concept within the integrative landslide early warning system (ILEWS). In *Landslides and Engineered Slopes. From the Past to the Future, Two Volumes + CD-ROM*. London: CRC Press.

Bensen, G. D., Ritzwoller, M. H., Barmin, M. P., Levshin, A. L., Lin, F., Moschetti, M. P., et al. (2007). Processing seismic ambient noise data to obtain reliable broad-band surface wave dispersion measurements. *Geophysical Journal International*, *169*(3), 1239–1260. https://doi.org/10.1111/j.1365-246X.2007.03374.x

Bergamo, P., Dashwood, B., Uhlemann, S., Swift, R., Chambers, J. E., Gunn, D. A., & Donohue, S. (2016). Time-lapse monitoring of climate effects on earthworks using surface waves. *Geophysics*, *81*(2), EN1–EN15. https://doi.org/10.1190/geo2015-0275.1

Bièvre, G., Jongmans, D., Winiarski, T., & Zumbo, V. (2012). Application of geophysical measurements for assessing the role of fissures in water infiltration within a clay landslide (Trièves area, French Alps). *Hydrological Processes*, *26*(14), 2128–2142. https://doi.org/10.1002/hyp.7986

Binley, A., Hubbard, S. S., Huisman, J. A., Revil, A., Robinson, D. A., Singha, K., & Slater, L. D. (2015). The emergence of hydrogeophysics for improved understanding of subsurface processes over multiple scales. *Water Resources Research*, *51*, 3837–3866. https://doi.org/10.1002/2015WR017016

Boyle, A., Wilkinson, P. B., Chambers, J. E., Meldrum, P. I., Uhlemann, S., & Adler, A. (2017). Jointly reconstructing ground motion and resistivity [0.1 em] for ERT-based slope stability monitoring. *Geophysical Journal International*, *212*, 1167–1182. https://doi.org/10.1093/gji/ggx453

Brückl, E., Brunner, F. K., Lang, E., Mertl, S., Müller, M., & Stary, U. (2013). The Gradenbach observatory—Monitoring deep-seated gravitational slope deformation by geodetic, hydrological, and seismological methods. *Landslides*, *10*(6), 815–829. https://doi.org/10.1007/s10346-013-0417-1

Brückl, E. & Mertl, S. (2006). Seismic monitoring of deep-seated mass movements.

Carrara, A., Cardinali, M., & Guzzetti, F. (1992). Uncertainty in assessing landslide hazard and risk. *ITC Journal*, *2*, 172–183.

Carrara, A., Crosta, G., & Frattini, P. (2003). Geomorphological and historical data in assessing landslide hazard. *Earth Surface Processes and Landforms*, *28*(10), 1125–1142. https://doi.org/10.1002/esp.545

Carrière, S. R., Jongmans, D., Chambon, G., Bièvre, G., Lanson, B., Bertello, L., et al. (2018). Rheological properties of clayey soils originating from flow-like landslides. *Landslides*, *15*(8), 1615–1630. https://doi.org/10.1007/s10346-018-0972-6

Cascini, L. (2008). Applicability of landslide susceptibility and hazard zoning at different scales. *Engineering Geology*, *102*(3-4), 164–177. https://doi.org/10.1016/j.enggeo.2008.03.016

Chambers, J. E., Meldrum, P. I., Wilkinson, P. B., Gunn, D., Uhlemann, S., Kuras, O., et al. (2016). Remote condition assessment of geotechnical assets using a new low-power ERT monitoring system. 22nd European Meeting of Environmental and Engineering Geophysics, Near Surface Geoscience.

Chambers, J. E., Meldrum, P. I., Wilkinson, P. B., Ward, W., Jackson, C., Matthews, B., et al. (2015). Spatial monitoring of groundwater drawdown and rebound associated with quarry dewatering using automated time-lapse electrical resistivity tomography and distribution guided clustering. *Engineering Geology*, *193*, 412–420. https://doi.org/10.1016/j.enggeo.2015.05.015

Chambers, J. E., Wilkinson, P. B., Kuras, O., Ford, J. R., Gunn, D. A., Meldrum, P. I., et al. (2011). Three-dimensional geophysical anatomy of an active landslide in Lias group mudrocks, Cleveland Basin, UK. *Geomorphology*, *125*(4), 472–484. https://doi.org/10.1016/j.geomorph.2010.09.017

Chambers, K., Kendall, J. M., Brandsberg-Dahl, S., & Rueda, J. (2010). Testing the ability of surface arrays to monitor microseismic activity. *Geophysical Prospecting*, *58*(5), 821–830. https://doi.org/10.1111/j.1365-2478.2010.00893.x

Chatelain, J.-L. (2004). Guidelines for the implementation of the H/V spectral ratio technique on ambient vibrations.

Colangelo, G., Lapenna, V., Perrone, A., Piscitelli, S., & Telesca, L. (2006). 2D self-potential tomographies for studying groundwater flows in the Varco d'Izzo landslide (Basilicata, southern Italy). *Engineering Geology*, *88*(3-4), 274–286. https://doi.org/10.1016/j.enggeo.2006.09.014

Craig, R. F. (2004). *Craig's Soil Mechanics* (7th ed.), London; New York, Spon: Taylor & Francis.

Crawford, M. M., & Bryson, L. S. (2018). Assessment of active landslides using field electrical measurements. *Engineering Geology*, *233*, 146–159. https://doi.org/10.1016/j.enggeo.2017.11.012

Cruden, D. M. & Varnes, D. J. (1996). Landslide types and processes.

Daley, T. M., Solbau, R. D., Ajo-Franklin, J. B., & Benson, S. M. (2007). Continuous active-source seismic monitoring of CO_2 injection in a brine aquifer. *Geophysics*, *72*(5), A57–A61. https://doi.org/10.1190/1.2754716

Daskalakis, E., Evangelidis, C. P., Garnier, J., Melis, N. S., Papanicolaou, G., & Tsogka, C. (2016). Robust seismic velocity change estimation using ambient noise recordings. *Geophysical Journal International*, *205*(3), 1926–1936. https://doi.org/10.1093/gji/ggw142

Deekshit, V. N., Ramesh, M. V., Indukala, P. K. & Nair, G. J. (2016) Smart geophone sensor network for effective detection of landslide induced geophone signals. International Conference on Communication and Signal Processing (ICCSP), 6–8 April 2016 2016.1565–1569.

Dou, S., Lindsey, N., Wagner, A. M., Daley, T. M., Freifeld, B., Robertson, M., et al. (2017). Distributed acoustic sensing for seismic monitoring of the near surface: A traffic-noise interferometry case study. *Scientific Reports*, *7*(1), 11620. https://doi.org/10.1038/s41598-017-11986-4

Everett, M. E. (2013). *Near-Surface Applied Geophysics*. New York: Cambridge University Press. https://doi.org/10.1017/CBO9781139088435

Fell, R. (1994). Landslide risk assessment and acceptable risk. *Canadian Geotechnical Journal*, *31*(2), 261–272. https://doi.org/10.1139/t94-031

Fell, R., Corominas, J., Bonnard, C., Cascini, L., Leroi, E., & Savage, W. Z. (2008). Guidelines for landslide susceptibility, hazard and risk zoning for land use planning. *Engineering Geology*, *102*(3-4), 85–98. https://doi.org/10.1016/j.enggeo.2008.03.022

Fiorucci, M., Iannucci, R., Martino, S., & Paciello, A. (2016). Detection of nanoseismic events related to slope instabilities in the quarry district of Coreno Ausonio (Italy). *Italian Journal of Engineering Geology and Environment*, *16*, 13.

Friedel, S., Thielen, A., & Springman, S. M. (2006). Investigation of a slope endangered by rainfall-induced landslides using 3D resistivity tomography and geotechnical testing. *Journal of Applied Geophysics*, *60*(2), 100–114. https://doi.org/10.1016/j.jappgeo.2006.01.001

Froude, M. J., & Petley, D. N. (2018). Global fatal landslide occurrence from 2004 to 2016. *Natural Hazards and Earth System Sciences*, *18*(8), 2161–2181. https://doi.org/10.5194/nhess-18-2161-2018

Gance, J., Malet, J. P., Supper, R., Sailhac, P., Ottowitz, D., & Jochum, B. (2016). Permanent electrical resistivity measurements for monitoring water circulation in clayey landslides. *Journal of Applied Geophysics*, *126*, 98–115. https://doi.org/10.1016/j.jappgeo.2016.01.011

Gariano, S. L., & Guzzetti, F. (2016). Landslides in a changing climate. *Earth-Science Reviews*, *162*, 227–252. https://doi.org/10.1016/j.earscirev.2016.08.011

Gill, J. C., & Malamud, B. D. (2014). Reviewing and visualizing the interactions of natural hazards. *Reviews of Geophysics*, *52*, 680–722. https://doi.org/10.1002/2013RG000445

Göktürkler, G., Balkaya, Ç., & Erhan, Z. (2008). Geophysical investigation of a landslide: The Altındağ landslide site, İzmir (western Turkey). *Journal of Applied Geophysics*, *65*(2), 84–96. https://doi.org/10.1016/j.jappgeo.2008.05.008

Gomberg, J., Bodin, P., Savage, W. Z., & Jackson, M. E. (1995). Landslide faults and tectonic faults, analogs?: The Slumgullion earthflow, Colorado. *Geology*, *23*(1), 41–44. https://doi.org/10.1130/0091-7613(1995)023<0041:LFATFA>2.3.CO;2

Gomberg, J., Schulz, W., Bodin, P., & Kean, J. (2011). Seismic and geodetic signatures of fault slip at the Slumgullion Landslide Natural Laboratory. *Journal of Geophysical Research*, *116*, B09404. https://doi.org/10.1029/2011JB008304

Grandjean, G., Cerdan, O., Richard, G., Cousin, I., Lagacherie, P., Tabbagh, A., et al. (2010). DIGISOIL: An integrated system of data collection technologies for mapping soil properties.

Grandjean, G., Hibert, C., Mathieu, F., Garel, E., & Malet, J.-P. (2009). Monitoring water flow in a clay-shale hillslope from geophysical data fusion based on a fuzzy logic approach. *Comptes Rendus Geoscience*, *341*(10-11), 937–948. https://doi.org/10.1016/j.crte.2009.08.003

Grelle, G. & Guadagno, F. M. (2009). Seismic refraction methodology for groundwater level determination: "Water seismic index." *Journal of Applied Geophysics, 68*, 301–320, 3. https://doi.org/10.1016/j.jappgeo.2009.02.001

Guzzetti, F., Carrara, A., Cardinali, M., & Reichenbach, P. (1999). Landslide hazard evaluation: A review of current techniques and their application in a multi-scale study, central Italy. *Geomorphology*, *31*(1-4), 181–216. https://doi.org/10.1016/S0169-555X(99)00078-1

Guzzetti, F., Mondini, A. C., Cardinali, M., Fiorucci, F., Santangelo, M., & Chang, K.-T. (2012). Landslide inventory maps: New tools for an old problem. *Earth-Science Reviews*, *112*(1-2), 42–66. https://doi.org/10.1016/j.earscirev.2012.02.001

Hack, R. (2000). Geophysics for slope stability. *Surveys in Geophysics*, *21*(4), 423–448. https://doi.org/10.1023/A:1006797126800
Haque, U., Blum, P., Da Silva, P. F., Andersen, P., Pilz, J., Chalov, S. R., et al. (2016). Fatal landslides in Europe. *Landslides*, *13*(6), 1545–1554. https://doi.org/10.1007/s10346-016-0689-3
Harba, P., & Pilecki, Z. (2017). Assessment of time–spatial changes of shear wave velocities of flysch formation prone to mass movements by seismic interferometry with the use of ambient noise. *Landslides*, *14*(3), 1225–1233. https://doi.org/10.1007/s10346-016-0779-2
Helmstetter, A., & Garambois, S. (2010). Seismic monitoring of Séchilienne rockslide (French Alps): Analysis of seismic signals and their correlation with rainfalls. *Journal of Geophysical Research*, *115*, F03016. https://doi.org/10.1029/2009JF001532
Hen-Jones, R. M., Hughes, P. N., Stirling, R. A., Glendinning, S., Chambers, J. E., Gunn, D. A., & Cui, Y. J. (2017). Seasonal effects on geophysical–geotechnical relationships and their implications for electrical resistivity tomography monitoring of slopes. *Acta Geotechnica*, *12*(5), 1159–1173. https://doi.org/10.1007/s11440-017-0523-7
Hibert, C., Malet, J. P., Bourrier, F., Provost, F., Berger, F., Bornemann, P., et al. (2017). Single-block rockfall dynamics inferred from seismic signal analysis. *Earth Surface Dynamics*, *5*(2), 283–292. https://doi.org/10.5194/esurf-5-283-2017
Hilley, G. E., Bürgmann, R., Ferretti, A., Novali, F., & Rocca, F. (2004). Dynamics of slow-moving landslides from permanent scatterer analysis. *Science*, *304*(5679), 1952–1955. https://doi.org/10.1126/science.1098821
Hruska, J., & Hubatka, F. (2000). Landslide investigation and monitoring by a high-performance ground penetrating radar system. 8th International Conference on Ground Penetrating Radar, SPIE, 6.
Hungr, O., Leroueil, S., & Picarelli, L. (2014). The Varnes classification of landslide types, an update. *Landslides*, *11*(2), 167–194. https://doi.org/10.1007/s10346-013-0436-y
Hutchinson, J. N., & Bhandari, R. K. (1971). Undrained loading, a fundamental mechanism of mudflows and other mass movements. *Géotechnique*, *21*(4), 353–358. https://doi.org/10.1680/geot.1971.21.4.353
Imposa, S., Grassi, S., Fazio, F., Rannisi, G., & Cino, P. (2017). Geophysical surveys to study a landslide body (north-eastern Sicily). *Natural Hazards*, *86*(S2), 327–343. https://doi.org/10.1007/s11069-016-2544-1
Intrieri, E., Gigli, G., Casagli, N., & Nadim, F. (2013). Brief communication "landslide early warning system: Toolbox and general concepts". *Natural Hazards and Earth System Sciences*, *13*(1), 85–90. https://doi.org/10.5194/nhess-13-85-2013
Intrieri, E., Gigli, G., Mugnai, F., Fanti, R., & Casagli, N. (2012). Design and implementation of a landslide early warning system. *Engineering Geology*, *147*, 124–136.
Jibson, R. W. 1993. Predicting earthquake-induced landslide displacements using Newmark's sliding block analysis. Transportation Research Record.
Jomard, H., Lebourg, T., Binet, S., Tric, E., & Hernandez, M. (2007). Characterization of an internal slope movement structure by hydrogeophysical surveying. *Terra Nova*, *19*(1), 48–57. https://doi.org/10.1111/j.1365-3121.2006.00712.x
Jomard, H., Lebourg, T., Guglielmi, Y., & Tric, E. (2010). Electrical imaging of sliding geometry and fluids associated with a deep seated landslide (La Clapière, France). *Earth Surface Processes and Landforms*, *35*, 588–599.
Jongmans, D., Baillet, L., Larose, E., Bottelin, P., Mainsant, G., Chambon, G., & Jaboyedoff, M. (2015). Application of ambient vibration techniques for monitoring the triggering of rapid landslides. In G. Lollino, D. Giordan, G. Crosta, J. Corominas, R. Azzam, J. Wasowski, & N. Sciarra (Eds.), *Engineering Geology for Society and Territory—Volume 2* (pp. 371–374). Cham, Switzerland: Springer International Publishing. https://doi.org/10.1007/978-3-319-09057-3_57
Jongmans, D., Bièvre, G., Renalier, F., Schwartz, S., Beaurez, N., & Orengo, Y. (2009). Geophysical investigation of a large landslide in glaciolacustrine clays in the Trièves area (French Alps). *Engineering Geology*, *109*(1-2), 45–56. https://doi.org/10.1016/j.enggeo.2008.10.005
Jongmans, D., & Garambois, S. (2007). Geophysical investigation of landslides: A review. *Bulletin de la Societe Geologique de France*, *178*(2), 101–112. https://doi.org/10.2113/gssgfbull.178.2.101
Kao, H., Kan, C.-W., Chen, R.-Y., Chang, C.-H., Rosenberger, A., Shin, T.-C., et al. (2012). Locating, monitoring, and characterizing typhoon-induced landslides with real-time seismic signals. *Landslides*, *9*(4), 557–563. https://doi.org/10.1007/s10346-012-0322-z
Kearey, P., Brooks, M., & Hill, I. (2001). *An Introduction to Geophysical Exploration*. Malden, MA: Blackwell Science.
Kirschbaum, D., Stanley, T., & Zhou, Y. (2015). Spatial and temporal analysis of a global landslide catalog. *Geomorphology*, *249*, 4–15. https://doi.org/10.1016/j.geomorph.2015.03.016
Kirschbaum, D. B., Adler, R., Hong, Y., Hill, S., & Lerner-Lam, A. (2010). A global landslide catalog for hazard applications: Method, results, and limitations. *Natural Hazards*, *52*(3), 561–575. https://doi.org/10.1007/s11069-009-9401-4
Kremers, S., Zimmermann, K., & Fleer, A. (2015). Geophysical and geodetical monitoring of slope movements at the Three Gorges dam area of the Yangtze River in China. In G. Lollino, D. Giordan, G. Crosta, J. Corominas, R. Azzam, J. Wasowski, & N. Sciarra (Eds.), *Engineering Geology for Society and Territory—Volume 2* (pp. 1415–1420). Cham, Switzerland: Springer International Publishing. https://doi.org/10.1007/978-3-319-09057-3_250
Lacroix, P., & Helmstetter, A. (2011). Location of seismic signals associated with microearthquakes and rockfalls on the Séchilienne landslide, French Alps. *Bulletin of the Seismological Society of America*, *101*(1), 341–353. https://doi.org/10.1785/0120100110
Le Roux, O., Jongmans, D., Kasperski, J., Schwartz, S., Potherat, P., Lebrouc, V., et al. (2011). Deep geophysical investigation of the large Séchilienne landslide (western Alps, France) and calibration with geological data. *Engineering Geology*, *120*(1-4), 18–31. https://doi.org/10.1016/j.enggeo.2011.03.004
Lebourg, T., Binet, S., Tric, E., Jomard, H., & El Bedoui, S. (2005). Geophysical survey to estimate the 3D sliding surface and the 4D evolution of the water pressure on part of a deep seated landslide. *Terra Nova*, *17*(5), 399–406. https://doi.org/10.1111/j.1365-3121.2005.00623.x
Lebourg, T., Hernandez, M., Zerathe, S., El Bedoui, S., Jomard, H., & Fresia, B. (2010). Landslides triggered factors analysed by time lapse electrical survey and multidimensional statistical approach. *Engineering Geology*, *114*(3-4), 238–250. https://doi.org/10.1016/j.enggeo.2010.05.001
Lecocq, T., Caudron, C., & Brenguier, F. (2014). MSNoise, a Python package for monitoring seismic velocity changes using ambient seismic noise. *Seismological Research Letters*, *85*(3), 715–726. https://doi.org/10.1785/0220130073
Lehmann, P., Gambazzi, F., Suski, B., Baron, L., Askarinejad, A., Springman, S. M., et al. (2013). Evolution of soil wetting patterns preceding a hydrologically induced landslide inferred from electrical resistivity survey and point measurements of volumetric water content and pore water pressure. *Water Resources Research*, *49*, 7992–8004. https://doi.org/10.1002/2013WR014560
Leroueil, S., Vaunat, J., Picarelli, L., Locat, J., Lee, H. & Faure, R. (1996), Geotechnical characterisation of slope movements. 7 International Symposium on Landslides. AA Balkema, 53–74.
Loke, M. H., Chambers, J. E., Rucker, D. F., Kuras, O., & Wilkinson, P. B. (2013). Recent developments in the direct-current geoelectrical imaging method. *Journal of Applied Geophysics*, *95*, 135–156. https://doi.org/10.1016/j.jappgeo.2013.02.017

Loke, M. H., Wilkinson, P. B., Chambers, J. E., & Meldrum, P. I. (2017). Rapid inversion of data from 2D resistivity surveys with electrode displacements. *Geophysical Prospecting*, *66*(3), 579–594.

Lotti, A., Saccorotti, G., Fiaschi, A., Matassoni, L., Gigli, G., Pazzi, V., & Casagli, N. (2015). Seismic monitoring of a rockslide: The Torgiovannetto quarry (central Apennines, Italy). In G. Lollino, D. Giordan, G. Crosta, J. Corominas, R. Azzam, J. Wasowski, & N. Sciarra (Eds.), *Engineering Geology for Society and Territory—Volume 2* (pp. 1537–1540). Cham, Switzerland: Springer International Publishing. https://doi.org/10.1007/978-3-319-09057-3_272

Lucas, D. R., Fankhauser, K., & Springman, S. M. (2017). Application of geotechnical and geophysical field measurements in an active alpine environment. *Engineering Geology*, *219*, 32–51. https://doi.org/10.1016/j.enggeo.2016.11.018

Luongo, R., Perrone, A., Piscitelli, S., & Lapenna, V. (2012). A prototype system for time-lapse electrical resistivity tomographies. *International Journal of Geophysics*, *2012*. https://doi.org/10.1155/2012/176895

Mainsant, G., Larose, E., Brönnimann, C., Jongmans, D., Michoud, C., & Jaboyedoff, M. (2012). Ambient seismic noise monitoring of a clay landslide: Toward failure prediction. *Journal of Geophysical Research*, *117*, F01030. https://doi.org/10.1029/2011JF002159

Malet, J. P., Van Asch, T. W. J., Van Beek, R., & Maquaire, O. (2005). Forecasting the behaviour of complex landslides with a spatially distributed hydrological model. *Natural Hazards and Earth System Sciences*, *5*(1), 71–85. https://doi.org/10.5194/nhess-5-71-2005

Manconi, A., & Giordan, D. (2015). Landslide early warning based on failure forecast models: The example of the Mt. de La Saxe rockslide, northern Italy. *Natural Hazards and Earth System Sciences*, *15*, 1639–1644.

Manconi, A., & Giordan, D. (2016). Landslide failure forecast in near-real-time. *Geomatics, Natural Hazards and Risk*, *7*(2), 639–648. https://doi.org/10.1080/19475705.2014.942388

Manconi, A., Picozzi, M., Coviello, V., De Santis, F., & Elia, L. (2016). Real-time detection, location, and characterization of rockslides using broadband regional seismic networks. *Geophysical Research Letters*, *43*, 6960–6967. https://doi.org/10.1002/2016GL069572

Martinez, K., Hart, J. K., Basford, P. J., Bragg, G. M., Ward, T., & Young, D. S. (2017). A geophone wireless sensor network for investigating glacier stick-slip motion. *Computers & Geosciences*, *105*, 103–112. https://doi.org/10.1016/j.cageo.2017.05.005

Mccann, D. M., & Forster, A. (1990). Reconnaissance geophysical methods in landslide investigations. *Engineering Geology*, *29*(1), 59–78. https://doi.org/10.1016/0013-7952(90)90082-C

Medina-Cetina, Z., & Nadim, F. (2008). Stochastic design of an early warning system. *Georisk: Assessment and Management of Risk for Engineered Systems and Geohazards*, *2*, 223–236.

Merritt, A. J., Chambers, J. E., Murphy, W., Wilkinson, P. B., West, L. J., Uhlemann, S., et al. (2018). Landslide activation behaviour illuminated by electrical resistance monitoring. *Earth Surface Processes and Landforms*, *43*(6), 1321–1334.

Merritt, A. J., Chambers, J. E., Wilkinson, P. B., West, L. J., Murphy, W., Gunn, D., & Uhlemann, S. (2016). Measurement and modelling of moisture—Electrical resistivity relationship of fine-grained unsaturated soils and electrical anisotropy. *Journal of Applied Geophysics*, *124*, 155–165. https://doi.org/10.1016/j.jappgeo.2015.11.005

Nakamura, Y. (1989). Method for dynamic characteristics estimation of subsurface using microtremor on the ground surface. *Quarterly Report of RTRI (Railway Technical Research Institute) (Japan)*, *30*, 25–33.

Olivier, G., Brenguier, F., De Wit, T., & Lynch, R. (2017). Monitoring the stability of tailings dam walls with ambient seismic noise. *The Leading Edge*, *36*, 350a1–350a6.

Öz, Y. (2015). Engineering seismology.

Ozaki, Y., Mikada, H., Goto, T. N., & Takekawa, J. (2014). The 3D self-potential inversion for the estimation of hydraulic parameters. *SEG Technical Program Expanded Abstracts*, 4539–4543.

Palis, E., Lebourg, T., Tric, E., Malet, J.-P., & Vidal, M. (2017). Long-term monitoring of a large deep-seated landslide (La Clapiere, south-east French Alps): Initial study. *Landslides*, *14*(1), 155–170. https://doi.org/10.1007/s10346-016-0705-7

Palis, E., Lebourg, T., Vidal, M., Levy, C., Tric, E., & Hernandez, M. (2017). Multiyear time-lapse ERT to study short- and long-term landslide hydrological dynamics. *Landslides*, *14*(4), 1333–1343. https://doi.org/10.1007/s10346-016-0791-6

Park, C. B., & Miller, R. D. (2008). Roadside passive multichannel analysis of surface waves (MASW). *Journal of Environmental and Engineering Geophysics*, *13*(1), 1–11. https://doi.org/10.2113/JEEG13.1.1

Parsekian, A. D., Singha, K., Minsley, B. J., Holbrook, W. S., & Slater, L. (2015). Multiscale geophysical imaging of the critical zone. *Reviews of Geophysics*, *53*, 1–26. https://doi.org/10.1002/2014RG000465

Partsinevelos, P., Kritikakis, G., Economou, N., Agioutantis, Z., Tripolitsiotis, A., Mertikas, S., & Vafidis, A. (2016). Integration of seismic and image data processing for rockfall monitoring and early warning along transportation networks. *Natural Hazards*, *83*(S1), 133–153. https://doi.org/10.1007/s11069-016-2462-2

Pasquet, S., Bodet, L., Longuevergne, L., Dhemaied, A., Camerlynck, C., Rejiba, F., & Guérin, R. (2015). 2D characterization of near-surface V_P/V_S: Surface-wave dispersion inversion versus refraction tomography. *Near Surface Geophysics*, *13*, 315–331.

Pennington, C., Freeborough, K., Dashwood, C., Dijkstra, T., & Lawrie, K. (2015). The National Landslide Database of Great Britain: Acquisition, communication and the role of social media. *Geomorphology*, *249*, 44–51. https://doi.org/10.1016/j.geomorph.2015.03.013

Perrone, A., Iannuzzi, A., Lapenna, V., Lorenzo, P., Piscitelli, S., Rizzo, E., & Sdao, F. (2004). High-resolution electrical imaging of the Varco d'Izzo earthflow (southern Italy). *Journal of Applied Geophysics*, *56*(1), 17–29. https://doi.org/10.1016/j.jappgeo.2004.03.004

Perrone, A., Lapenna, V., & Piscitelli, S. (2014). Electrical resistivity tomography technique for landslide investigation: A review. *Earth-Science Reviews*, *135*, 65–82. https://doi.org/10.1016/j.earscirev.2014.04.002

Pescaroli, G. & Alexander, D. (2015). A definition of cascading disasters and cascading effects: Going beyond the "toppling dominos" metaphor. Planet@ Risk, 3.

Petley, D. (2012). Global patterns of loss of life from landslides. *Geology*, *40*(10), 927–930. https://doi.org/10.1130/G33217.1

Planès, T., Mooney, M. A., Rittgers, J. B. R., Parekh, M. L., Behm, M., & Snieder, R. (2016). Time-lapse monitoring of internal erosion in earthen dams and levees using ambient seismic noise. *Géotechnique*, *66*(4), 301–312. https://doi.org/10.1680/jgeot.14.P.268

Poli, P. (2017). Creep and slip: Seismic precursors to the Nuugaatsiaq landslide (Greenland). *Geophysical Research Letters*, *44*, 8832–8836. https://doi.org/10.1002/2017GL075039

Provost, F., Hibert, C., & Malet, J. P. (2017). Automatic classification of endogenous landslide seismicity using the random Forest supervised classifier. *Geophysical Research Letters*, *44*, 113–120. https://doi.org/10.1002/2016GL070709

Ramesh, M. V. (2014). Design, development, and deployment of a wireless sensor network for detection of landslides. *Ad Hoc Networks*, *13*(part a), 2–18.

Ramesh, M. V., & Rangan, V. P. (2014). Data reduction and energy sustenance in multisensor networks for landslide monitoring. *IEEE Sensors Journal*, *14*(5), 1555–1563. https://doi.org/10.1109/JSEN.2013.2296611

Renalier, F., Bievre, G., Jongmans, D., Campillo, M., & Bard, P. Y. (2010). Clayey landslide investigations using active and passive V-S measurements. In R. D. Miller, J. H. Bradford, & K. Holliger (Eds.), *Advances in Near-Surface Seismology and Ground-Penetrating Radar* (pp. 397–413). Washington, DC.

Renalier, F., Jongmans, D., Campillo, M., & Bard, P. Y. (2010). Shear wave velocity imaging of the Avignonet landslide (France) using ambient noise cross correlation. *Journal of Geophysical Research*, *115*, F03032. https://doi.org/10.1029/2009JF001538

Rosso, R., Rulli, M. C., & Vannucchi, G. (2006). A physically based model for the hydrologic control on shallow landsliding. *Water Resources Research*, *42*, W06410. https://doi.org/10.1029/2005WR004369

Safeland (2012). Deliverable 4.8: Guidelines for landslide monitoring and early warning systems in Europe—Design and required technology. *Living with landslide risk in Europe: Assessment, effects of global change, and risk management strategies*. Revision 1 ed.

Salvermoser, J., Hadziioannou, C., & Stähler, S. C. (2015). Structural monitoring of a highway bridge using passive noise recordings from street traffic. *The Journal of the Acoustical Society of America*, *138*(6), 3864–3872. https://doi.org/10.1121/1.4937765

Sastry, R. G., & Mondal, S. K. (2013). Geophysical characterization of the Salna sinking zone, Garhwal Himalaya, India. *Surveys in Geophysics*, *34*(1), 89–119. https://doi.org/10.1007/s10712-012-9206-y

Schrott, L., & Sass, O. (2008). Application of field geophysics in geomorphology: Advances and limitations exemplified by case studies. *Geomorphology*, *93*(1-2), 55–73. https://doi.org/10.1016/j.geomorph.2006.12.024

Skempton, A., & Hutchinson, J. (1969). Stability of natural slopes and embankment foundations. Soil Mech & Fdn Eng Conf Proc/Mexico/.

Spiker, E. C. & Gori, P. L. (2003). National landslide hazards mitigation strategy: A framework for loss reduction. *Circular*. - ed.

Springman, S. M., Thielen, A., Kienzler, P., & Friedel, S. (2013). A long-term field study for the investigation of rainfall-induced landslides. *Géotechnique*, *63*(14), 1177–1193. https://doi.org/10.1680/geot.11.P.142

Stork, A. L., Allmark, C., Curtis, A., Kendall, J. M., & White, D. J. (2018). Assessing the potential to use repeated ambient noise seismic tomography to detect CO_2 leaks: Application to the Aquistore storage site. *International Journal of Greenhouse Gas Control*, *71*, 20–35. https://doi.org/10.1016/j.ijggc.2018.02.007

Supper, R., Ottowitz, D., Jochum, B., Kim, J. H., Römer, A., Baron, I., et al. (2014). Geoelectrical monitoring: An innovative method to supplement landslide surveillance and early warning. *Near Surface Geophysics*, *12*, 133–150.

Suriñach, E., Vilajosana, I., Khazaradze, G., Biescas, B., Furdada, G., & Vilaplana, J. M. (2005). Seismic detection and characterization of landslides and other mass movements. *Natural Hazards and Earth System Sciences*, *5*(6), 791–798. https://doi.org/10.5194/nhess-5-791-2005

Terzaghi, K. (1943). *Theoretical Soil Mechanics*. London and New York: John Wiley. https://doi.org/10.1002/9780470172766

Terzaghi, K., Peck, R. B., Mesri, G., & Knovel (1996). *Soil Mechanics in Engineering Practice*. New York: John Wiley.

Toll, D. G., Lourenço, S. D. N., Mendes, J., Gallipoli, D., Evans, F. D., Augarde, C. E., et al. (2011). Soil suction monitoring for landslides and slopes. *Quarterly Journal of Engineering Geology and Hydrogeology*, *44*(1), 23–33. https://doi.org/10.1144/1470-9236/09-010

Tonnellier, A., Helmstetter, A., Malet, J.-P., Schmittbuhl, J., Corsini, A., & Joswig, M. (2013). Seismic monitoring of soft-rock landslides: The super-Sauze and Valoria case studies. *Geophysical Journal International*, *193*(3), 1515–1536. https://doi.org/10.1093/gji/ggt039

Travelletti, J., Sailhac, P., Malet, J. P., Grandjean, G., & Ponton, J. (2012). Hydrological response of weathered clay-shale slopes: Water infiltration monitoring with time-lapse electrical resistivity tomography. *Hydrological Processes*, *26*(14), 2106–2119. https://doi.org/10.1002/hyp.7983

Uhlemann, S. (2018). Geoelectrical monitoring of moisture driven processes in natural and engineered slopes. ETH Zurich.

Uhlemann, S., Chambers, J., Wilkinson, P., Maurer, H., Merritt, A., Meldrum, P., et al. (2017). Four-dimensional imaging of moisture dynamics during landslide reactivation. *Journal of Geophysical Research: Earth Surface*, *122*, 398–418. https://doi.org/10.1002/2016JF003983

Uhlemann, S., Hagedorn, S., Dashwood, B., Maurer, H., Gunn, D., Dijkstra, T., & Chambers, J. (2016). Landslide characterization using *P*- and *S*-wave seismic refraction tomography—The importance of elastic moduli. *Journal of Applied Geophysics*, *134*, 64–76. https://doi.org/10.1016/j.jappgeo.2016.08.014

Uhlemann, S., Smith, A., Chambers, J., Dixon, N., Dijkstra, T., Haslam, E., et al. (2016). Assessment of ground-based monitoring techniques applied to landslide investigations. *Geomorphology*, *253*, 438–451. https://doi.org/10.1016/j.geomorph.2015.10.027

Van Westen, C. J., Van Asch, T. W. J., & Soeters, R. (2006). Landslide hazard and risk zonation—Why is it still so difficult? *Bulletin of Engineering Geology and the Environment*, *65*(2), 167–184. https://doi.org/10.1007/s10064-005-0023-0

Walter, M., Arnhardt, C., & Joswig, M. (2012). Seismic monitoring of rockfalls, slide quakes, and fissure development at the super-Sauze mudslide, French Alps. *Engineering Geology*, *128*, 12–22. https://doi.org/10.1016/j.enggeo.2011.11.002

Walter, M., Gomberg, J., Schulz, W., Bodin, P., & Joswig, M. (2013). Slidequake generation versus viscous creep at Softrock-landslides: Synopsis of three different scenarios at Slumgullion landslide, Heumoes slope, and super-Sauze mudslide slidequake generation vs viscous creep at Softrock-landslides. *Journal of Environmental and Engineering Geophysics*, *18*(4), 269–280. https://doi.org/10.2113/JEEG18.4.269

Walter, M., & Joswig, M. (2008). Seismic monitoring of fracture processes generated by a creeping landslide in the Vorarlberg Alps. *First Break*, *26*, 131–135.

Walter, M., Niethammer, U., Rothmund, S., & Joswig, M. (2009). Joint analysis of the super-Sauze (French Alps) mudslide by nanoseismic monitoring and UAV-based remote sensing. *First Break*, *27*, 75–82.

Walter, M., Walser, M., & Joswig, M. (2011). Mapping rainfall-triggered slidequakes and seismic landslide-volume estimation at Heumoes slope all rights reserved. No part of this periodical may be reproduced or transmitted in any form or by any means, electronic or mechanical, including photocopying, recording, or any information storage and retrieval system, without permission in writing from the publisher. *Vadose Zone Journal*, *10*, 487–495.

Wapenaar, K., Draganov, D., Snieder, R., Campman, X., & Verdel, A. (2010). Tutorial on seismic interferometry: Part 1—Basic principles and applications. *Geophysics*, *75*, 75A195–75A209.

Ward, W. O. C., Wilkinson, P. B., Chambers, J. E., Nilsson, H., Kuras, O., & Bai, L. (2016). Tracking tracer motion in a 4-D electrical resistivity tomography experiment. *Water Resources Research*, *52*, 4078–4094. https://doi.org/10.1002/2015WR017958

Waxman, M. H., & Smits, L. (1968). Electrical conductivities in oil-bearing shaly sands. *Society of Petroleum Engineers Journal*, *8*(02), 107–122. https://doi.org/10.2118/1863-A

Wilkinson, P., Chambers, J., Uhlemann, S., Meldrum, P., Smith, A., Dixon, N., & Loke, M. H. (2016). Reconstruction of landslide movements by inversion of 4-D electrical resistivity tomography monitoring data. *Geophysical Research Letters*, *43*, 1166–1174. https://doi.org/10.1002/2015GL067494

Wilkinson, P. B., Chambers, J. E., Meldrum, P. I., Gunn, D. A., Ogilvy, R. D., & Kuras, O. (2010). Predicting the movements of permanently installed electrodes on an active landslide using time-lapse geoelectrical resistivity data only. *Geophysical Journal International*, *183*(2), 543–556. https://doi.org/10.1111/j.1365-246X.2010.04760.x

Wilkinson, P. B., Uhlemann, S., Chambers, J. E., Meldrum, P. I., & Loke, M. H. (2015). Development and testing of displacement inversion to track electrode movements on 3-D electrical resistivity tomography monitoring grids. *Geophysical Journal International*, *200*(3), 1566–1581. https://doi.org/10.1093/gji/ggu483

Xu, D., Hu, X.-Y., Shan, C.-L., & Li, R.-H. (2016). Landslide monitoring in southwestern China via time-lapse electrical resistivity tomography. *Applied Geophysics*, *13*(1), 1–12. https://doi.org/10.1007/s11770-016-0543-3